Atmos. Chem. Phys., 18, 15125–15144, 2018
https://doi.org/10.5194/acp-18-15125-2018

Atmospheric Chemistry and Physics
Open Access
EGU

Diurnal variation of aerosol optical depth and $PM_{2.5}$ in South Korea: a synthesis from AERONET, satellite (GOCI), KORUS-AQ observation, and the WRF-Chem model

Elizabeth M. Lennartson[1], Jun Wang[1], Juping Gu[2], Lorena Castro Garcia[1], Cui Ge[1], Meng Gao[1,3], Myungje Choi[4], Pablo E. Saide[5], Gregory R. Carmichael[1], Jhoon Kim[4], and Scott J. Janz[6]

[1]Department of Chemical and Biochemical Engineering, Center for Global and Regional Environmental Research, University of Iowa, Iowa City, Iowa, USA
[2]Department of Electrical Engineering, Nantong University, Nantong, China
[3]School of Engineering and Applied Sciences, Harvard University, Cambridge, Massachusetts, USA
[4]Department of Atmospheric Science, Yonsei University, Seoul, Republic of Korea
[5]Department of Atmospheric and Oceanic Sciences, Institute of the Environment and Sustainability, University of California, Los Angeles, California, USA
[6]Lab for Atmospheric Chemistry and Dynamics, Code 614, NASA Goddard Space Flight Center, Greenbelt, Maryland, USA

Correspondence: Jun Wang (jun-wang-1@uiowa.edu) and Elizabeth M. Lennartson (elizabeth-lennartson@uiowa.edu)

Received: 15 April 2018 – Discussion started: 28 May 2018
Revised: 6 September 2018 – Accepted: 10 September 2018 – Published: 22 October 2018

Abstract. Spatial distribution of diurnal variations of aerosol properties in South Korea, both long term and short term, is studied by using 9 AERONET (AErosol RObotic NETwork) sites from 1999 to 2017 and an additional 10 sites during the KORUS-AQ (Korea–United States Air Quality) field campaign in May and June of 2016. The extent to which the WRF-Chem (Weather Research and Forecasting coupled with Chemistry) model and the GOCI (Geostationary Ocean Color Imager) satellite retrieval can describe these variations is also analyzed. On a daily average, aerosol optical depth (AOD) at 550 nm is 0.386 and shows a diurnal variation of 20 to −30 % in inland sites, which is larger than the AOD of 0.308 and diurnal variation of ±20 % seen in coastal sites. For all the inland and coastal sites, AERONET, GOCI, and WRF-Chem, and observed $PM_{2.5}$ (particulate matter with aerodynamic diameter less than 2.5 µm) data generally show dual peaks for both AOD and $PM_{2.5}$, one in the morning (often at ∼ 08:00–10:00 KST, Korea Standard Time, especially for $PM_{2.5}$) and another in the early afternoon (∼ 14:00 KST, albeit for $PM_{2.5}$ this peak is smaller and sometimes insignificant). In contrast, Ångström exponent values in all sites are between 1.2 and 1.4 with the exception of the inland rural sites having smaller values near 1.0 during the early morning hours. All inland sites experience a pronounced increase in the Ångström exponent from morning to evening, reflecting an overall decrease in particle size in daytime. To statistically obtain the climatology of diurnal variation of AOD, a minimum requirement of ∼ 2 years of observation is needed in coastal rural sites, twice as long as that required for the urban sites, which suggests that the diurnal variation of AOD in an urban setting is more distinct and persistent. While Korean GOCI satellite retrievals are able to consistently capture the diurnal variation of AOD (although it has a systematically low bias of 0.04 on average and up to 0.09 in later afternoon hours), WRF-Chem clearly has a deficiency in describing the relative change of peaks and variations between the morning and afternoon, suggesting further studies for the diurnal profile of emissions. Furthermore, the ratio between $PM_{2.5}$ and AOD in WRF-Chem is persistently larger than the observed counterparts by 30 %–50 % in different sites, but spatially no consistent diurnal variation pattern of this ratio can be found. Overall, the relatively small diurnal variation of $PM_{2.5}$ is in high contrast with large AOD diurnal variation, which suggests the large diurnal variation of AOD–$PM_{2.5}$ relationships (with the $PM_{2.5}$ / AOD ratio being largest in the early morning, decreasing around noon, and increasing in late afternoon) and, therefore, the need to use AOD from geosta-

tionary satellites to constrain either modeling or estimate of surface $PM_{2.5}$ for air quality application.

1 Introduction

Aerosols, both natural and anthropogenic, play an important role in air quality and the climate. They are involved in pollution events, and they have a direct and indirect role in modifying the Earth's radiation budget and properties of cloud and precipitation, respectively (Kaufman et al., 2002). Aerosols also lead to acute and chronic health effects due to their small size and ability to be inhaled through the respiratory tract to the lungs' alveoli (Pope et al., 2002). As the world continues to industrialize and increase in population (especially in developing countries), it is imperative to understand and mitigate the effects of pollutants on air quality, climate, and human health, in various spatial and temporal scales.

The United States' air quality index (AQI) is monitored on a daily basis to inform the population on how clean or polluted the air in their local area is. The particulate matter (PM) AQI is calculated from "the ratio between 24 h average of the measured dry particulate mass and the National Ambient Air Quality Standard (NAAQS)" (Wang and Christopher, 2003). For clean conditions, the 24-hour average NAAQS for fine particulate matter ($PM_{2.5}$, or particulate matter with aerodynamic diameter less than 2.5 µm) must be below 35 µg m^{-3}, which is 10 µg m^{-3} higher than the World Health Organization's (WHO) recommendation of 25 µg m^{-3} (EPA, 2016; WHO, 2006). Due its health implications and crucial role in determining daily air quality levels, it is of utmost importance to effectively monitor and predict 24 h average $PM_{2.5}$ concentrations.

$PM_{2.5}$ concentrations are typically measured from surface monitors. In the United States, there are roughly 600 continuous (hourly) monitors spread throughout the country and managed by federal, state, local, and tribal agencies (EPA, 2008). These monitors provide invaluable information regarding $PM_{2.5}$ levels 24 times per day and are not affected by weather conditions; particle-bound water included in the sampled air is removed by heating at a constant temperature (usually at 50 °C) inside the monitoring instrument (Wang et al., 2006). However, disadvantages include the fact that they do not represent pollution over large spatial areas. Furthermore, many populated locations in the world do not have a single monitor in their vicinity (Christopher and Gupta, 2010).

To gap fill between monitoring sites and provide estimates at locations around the world, recent research has focused on using satellite aerosol optical depth (AOD) to predict ground $PM_{2.5}$ concentrations. An early study by Wang and Christopher (2003) relied on a linear relationship to investigate the Moderate Resolution Imaging Spectroradiometer (MODIS) AOD and 24 h average and monthly average $PM_{2.5}$ concentrations. Other efforts have combined the use of satellite AOD with local scaling factors from global chemistry transport models; columnar NO_2; and factors such as the planetary boundary height, the temperature inversion layer, relative humidity, season, and site location (Liu et al., 2004, 2005; Ma et al., 2016; van Donkelaar et al., 2010; Zang et al., 2017; Zheng et al., 2016; Qu et al., 2016). A review by Hoff and Christopher (2009) summarizes that "the satellite precision in measuring AOD is ±20 % and the prediction of $PM_{2.5}$ concentrations from these values is ±30 % in the most careful studies."

Since air quality is often assessed with daily (24 h) or annual averages of surface $PM_{2.5}$, while the polar-orbiting satellite only provides AOD retrieval once per day for a given location (Wang et al., 2016), recent research has integrated AOD from geostationary satellites into the surface $PM_{2.5}$ analysis because a geostationary satellite can provide multiple measurements of AOD per day for a given a location (Wang et al., 2003a; b), thereby better constraining the diurnal variation of $PM_{2.5}$ for estimating 24-hour average $PM_{2.5}$ (Xu et al., 2015).

Here, we study the diurnal variation of $PM_{2.5}$ and AOD and evaluate such variations for air quality applications by focusing on a 6-week-long (April–June) air quality campaign in KORUS-AQ (Korea–United States Air Quality) and the long-term AERONET (AErosol RObotic NETwork) sites in South Korea. The campaign is the first of its kind in east Asia, involving international collaborations, integrated aircraft, surface and satellite data, and air quality models to assess urban, rural, and coastal air quality and its controlling factors. In this study, we first investigate the long-term AOD diurnal variation for various South Korean ground sites and then focus our analysis to the KORUS-AQ AOD diurnal variation as described by chemistry transport model and satellite and surface observations. By centering AOD diurnal variation in our analysis, this study seeks to address the following questions:

1. What is the climatology of AOD and its wavelength-dependent (Ångström exponent) diurnal variation in South Korea, both spatially and spectrally? How long should the ground measurement record be to derive the climatology of AOD diurnal variation?

2. To what degree can AOD diurnal variation be captured by GOCI (Geostationary Ocean Color Imager) and a chemistry transport model WRF-Chem (Weather Research and Forecasting coupled with Chemistry)?

3. What is the diurnal variation of surface $PM_{2.5}$? How well is the diurnal variation of the $PM_{2.5}$–AOD relationship captured by WRF-Chem?

The rest of the paper is organized as follows: Section 2 gives a brief overview of previous studies and the motivation for this research. Section 3 details the datasets used in this study,

and Sect. 4 contains the methods and analysis of the study. Section 5 closes the paper with a summary and the main conclusions.

2 Background and motivation

2.1 Diurnal variation AOD and Ångström exponent

The study of AOD diurnal variation dates back to the late 1960s but did not gain momentum until near the turn of the century (Barteneva et al., 1967; Panchenko et al., 1999; Peterson et al., 1981; Pinker et al., 1994). Peterson et al. (1981) found the AOD at Raleigh, North Carolina, to have an early afternoon maxima at 13:00–14:00 LT (local time) during the 1969–1975 study period. Pinker et al. (1994) showed that AOD in sub-Saharan Africa increased throughout the day in December 1987 while the January 1989 data showed maxima at 13:00 LT and minima at 10:00 and 16:00 LT. As recent as the early 2000s, the science community agreed that the "diurnal effects are largely unknown and little studied due to the paucity of data" (Smirnov et al., 2002).

Most diurnal variation of AOD research stemmed from the analysis of aerosol radiative forcing, which requires the knowledge of the diurnal distribution of key aerosol properties such as AOD, the single scattering albedo, and the asymmetry factor (Kassianov et al., 2013; Kuang et al., 2015; Wang et al., 2003b). Two early studies developed an algorithm to retrieve AOD diurnal variation from geostationary satellites over water and showed strong AOD diurnal variation during long-range aerosol transport events; Wang et al. (2003b) used April 2001 hourly data over water from the GMS (Geostationary Meteorological Satellite) imager and Wang et al. (2003a) used half-hourly data in July 2000 from the GOES-8 (Geostationary Operational Environmental Satellite) satellite during the ACE-Asia and PRIDE (Puerto Rico Dust Experiment) campaigns. Consistent with AERONET observations, the GOES-8 retrieval over Puerto Rico showed the dust AOD diurnal variation's noontime minimum and early morning or late afternoon maximum. Subsequent work by Wang et al. (2004) investigated the Taklimakan and Gobi dust regions in China using 1999–2000 AOD data from a nearby airport's Sun photometer. They found a seasonally invariant diurnal change of more than $\pm 10\,\%$ for dust AOD. Their results aligned with similar past studies which found the diurnal variation of dust aerosols to be $\pm < 5\,\%$–$15\,\%$ depending on the AERONET site's location and distance from a dust source region (Kaufman et al., 2000; Levin et al., 1980; Wang et al., 2003a). However, on a daily basis, the day-to-day variation of AOD can be distinct, up to 150 %, and both daily diurnal variation changes and relative departures of AOD from the daily mean are of up to 20 % (Kassianov et al., 2013; Kuang et al., 2015). Furthermore, using long-term Sun-photometer data from the China Aerosol Remote Sensing Network (CARSNET), Song et al. (2018) showed that AOD diurnal variation can be up to 30 % with a peak around noon in northwest China and a steady increase of 40 % from early morning to late afternoon in the northern China plains.

While AOD diurnal variation has been analyzed by several past studies, few studies examined the diurnal variation of the Ångström exponent. Wang et al. (2004) showed that the Ångström exponent on average has a diurnal variation of 30 % (with minima in the mid-afternoon) in the dust source region of the Gobi Desert. Globally, Kaufman et al. (2000) showed the ratio of the Ångström exponent at Terra satellite overpass time with respect to the daily mean is close 1 in 60 % of days for the AERONET sites from 1993 to 1999, and they clearly showed that the diurnal variation of the Ångström exponent is much larger than the counterpart of AOD. Recently, Song et al. (2018) also showed that the diurnal variation of the Ångström exponent is $\sim 15\,\%$ in southwest China, with minima in the mid-afternoon, and less than 10 % in northern China plains.

Overall, research based on limited ground-based observations has shown that, on a global and annual scale, the AOD diurnal variation exists, albeit relatively small. On a daily and local scale, AOD and Ångström exponent diurnal variations are significant, which calls upon the need of geostationary satellite measurements for both air quality and climate studies. Much less studied is the diurnal variation of the Ångström exponent. Newer geostationary satellites may play an important role for the future generation of AOD diurnal variation studies.

2.2 $PM_{2.5}$ diurnal variation

In addition to AOD diurnal variation, studies have also investigated the diurnal variation of $PM_{2.5}$. Epidemiological studies focused on the mass, size, spatial and temporal variability, and chemical composition of PM to investigate the complex sources and evolution of aerosols in the atmosphere (Fine et al., 2004; Sun et al., 2013; Wittig et al., 2004). In many of these studies, tracer species of primary aerosols and possible components of secondary organic aerosols were the main focus (Edgerton et al., 2006; Querol et al., 2001; Sun et al., 2013; Wittig et al., 2004).

Regarding diurnal variation of $PM_{2.5}$ mass, studies have found different results for various locations around the world. Querol et al. (2001) used data from June 1999 to June 2000 and found Barcelona's (Spain) diurnal variation of $PM_{2.5}$ in all four seasons to be characterized by an increase from the late afternoon to midnight. This trend was more pronounced in winter and autumn since the concentrations were higher from late afternoon to midnight in fall/winter relative to the spring/summer values.

In the United States, early studies have focused on the Los Angeles, Pittsburgh, and general southeast US areas. Fine et al. (2004) chose two sites, an urban one located at the University of Southern California (USC) and a rural one in River-

side, and studied the diurnal variation for 1 week in the summertime and 1 week in the wintertime. The USC site had a summer peak in the morning and midday with a winter peak in the morning. The Riverside site experienced a summer peak in the morning and a winter peak in the overnight hours. The winter results were attributed to the boundary layer temperature inversion that forms throughout the day over the area. A few years later in Pittsburgh, Wittig et al. (2004) found no clear $PM_{2.5}$ diurnal variability due to the combined effect of particulate matter species being transported to the area versus generated locally. Additionally, they concluded that the daily changes in $PM_{2.5}$ concentrations could be "attributed to the major components of the [particulate] mass, namely the sulfate". Data from the 1998–1999 Southeastern Aerosol and Characterization Study (SEARCH) was used by Edgerton et al. (2006) at four pairs of urban–rural sites. They established the following three main $PM_{2.5}$ temporal variation patterns: large values of >40–$50\,\mu g\,m^{-3}$ that occurred on timescales of a few hours, buildup occurring over several days and then returning to normal levels, and enhancements during the summer of similar magnitude as the monthly or quarterly averages. Their four sites had similar diurnal variations characterized by maxima at 06:00–08:00 LT and again from 18:00 to 21:00 LT, similar to those results found by Wang and Christopher (2003) at seven sites in Alabama. In South Korea, Ghim et al. (2015) showed that $PM_{2.5}$ average concentration in Seoul in 2002–2008 peaks at 09:00 KST (Korea Standard Time) and again around midnight, but such typical diurnal variation can sometimes be affected by long-range transport of dust. Similar diurnal variation for PM_{10} was also found by Yoo et al. (2015) over the southern Korean Peninsula, although its peak at daytime lagged behind that of $PM_{2.5}$ by 1 h, which is found in Ghim et al. (2015). Furthermore, both Ghim et al. (2015) and Yoo et al. (2015) showed that PM concentrations can significantly vary with space and time. Hence, in order to understand the potency and effects of the individual chemical species and $PM_{2.5}$ as a whole, it is urgently necessary to increase the amount of long-term measurements available and investigate other methods such as satellite remote sensing that can be used to assist with characterizing $PM_{2.5}$ concentrations and diurnal variation.

2.3 Diurnal variation of the AOD–$PM_{2.5}$ relationship

Recently, studies have focused on using satellite measurements of AOD in order to predict ground-level $PM_{2.5}$ concentrations in addition to investigating the diurnal variations of both components. An early study examined how well MODIS AOD correlated with 24 h average and monthly average $PM_{2.5}$ using a linear relationship and found linear correlation coefficients of 0.7 and 0.9, respectively. Additionally, when the linear relationship used the 24 h average $PM_{2.5}$ concentrations, MODIS AOD quantitatively estimated $PM_{2.5}$ AQI categories with typical errors of $\pm 10\,\%$ (in terms of capturing AQI variability) in cloud-free conditions (Wang and Christopher, 2003).

Other efforts have used satellite AOD in combination with additional factors to improve the prediction of ground-level $PM_{2.5}$, such as the planetary boundary layer height, relative humidity, season, and the geographical characteristics of the monitoring sites (Liu et al., 2005; Qu et al., 2016). Similarly, Gupta et al. (2006) found a strong dependence on aerosol concentration, relative humidity, fractional cloud cover, and the mixing layer height when analyzing the relationship between MODIS AOD and ground-level $PM_{2.5}$. They concluded the importance of local wind patterns for identifying the pollutant sources and, overall, high correlations can occur for the following four conditions: cloud-free, low boundary layer heights, AOD larger than 0.1, and low relative humidity.

Xu et al. (2015) used GOCI AOD in cloud-free days and a global chemistry transport model (GEOS-Chem or Goddard Earth Observing System with Chemistry) to find significant agreement between the derived $PM_{2.5}$ and the ground measured $PM_{2.5}$ for both the annual and monthly averages over eastern China. Incorporating AOD data from GOCI, a geostationary satellite, provided improvement for GEOS-Chem, a global chemistry transport model, to estimate ground-level $PM_{2.5}$ for a highly populated and polluted region of the world on a fine spatial resolution. When comparing their results to MODIS-AOD-derived $PM_{2.5}$, they found better agreement using their model with an R^2 value of 0.66. However, in their study, only daytime-averaged AOD from both GEOS-Chem and GOCI AOD is used as their study is concerned with monthly and annual timescales.

Hence, one common theme throughout most of the past research, with the exception of Xu et al. (2015), is the use of AOD data from low-Earth-orbiting (LEO) satellites to establish the AOD–$PM_{2.5}$ relationship. However, all the studies have relied on the model-simulated diurnal variation of the AOD–$PM_{2.5}$ relationship to convert satellite-based AOD (often once per day) to surface $PM_{2.5}$. An integrated analysis of diurnal variation of AOD, $PM_{2.5}$, and their relationship, with unprecedented observations from field campaigns, is overdue.

3 Study area and data

Over the last 40 years, South Korea has experienced an extensive list of air quality improvements for constituents such as lead, sulfur dioxide, and PM_{10} (Ministry of Environment, 2016). In 2015, they introduced a standard on $PM_{2.5}$, and, due to its recent implementation, the historical trends of $PM_{2.5}$ are not well established. Han et al. (2011) suggests that, prior to 2005, $PM_{2.5}$ annual averages either increased or remained constant in rural Chuncheon, South Korea. However, there has been a gradual decrease in the annual averages in Seoul since 2005, although the decreases have not

been continuous (Ahmed et al., 2015; Ghim et al., 2015; Lee, 2014). Annual averages have ranged from 33.5 $\mu g\,m^{-3}$ in 2004 to 21.9 $\mu g\,m^{-3}$ in 2012, but the most recent patterns have been difficult to interpret (Ahmed et al., 2015). Also, since the $PM_{2.5}$ concentrations discussed above were from research studies based only in the Seoul region, the aforementioned findings may not be fully applicable to South Korea as a whole. For this study, we will use all the AERONET data collected over South Korea since the early 1990s, as well as rich datasets collected during KORUS-AQ including an additional 10 AERONET sites, GOCI data, and WRF-Chem modeling data.

3.1 AERONET

The AERONET sites provide "long-term, continuous, and readily accessible" (NASA, 2018) aerosol data, with AOD and the Ångström exponent being two of the available parameters from the direct Sun measurements. Sequences are made in eight spectral bands between 340 and 1020 nm while the diffuse Sun measurements are made at 440, 670, 870, and 1020 nm (Holben et al., 1998). The version 2, level 2 quality level data are used for this study, which implies that the data are cloud-screened and quality-assured following the procedures detailed in Smirnov et al. (2000). To compare the AERONET AOD values to those commonly used by other data platforms such as satellites and models, the AOD at 550 nm is calculated by using the corresponding Ångström exponent derived from AOD at 440 and 870 nm .

At the time of last access to the AERONET database in July 2017, the stations listed in Table 1 had version 2, level 2 data available. These stations were further grouped into the following four land classifications: coastal urban, coastal rural, inland urban, and inland rural. Each site's classification membership is represented in Fig. 1a and b by its marker. The same marker color schemes are also used in other figures to correspondingly denote AOD diurnal variation at each individual site.

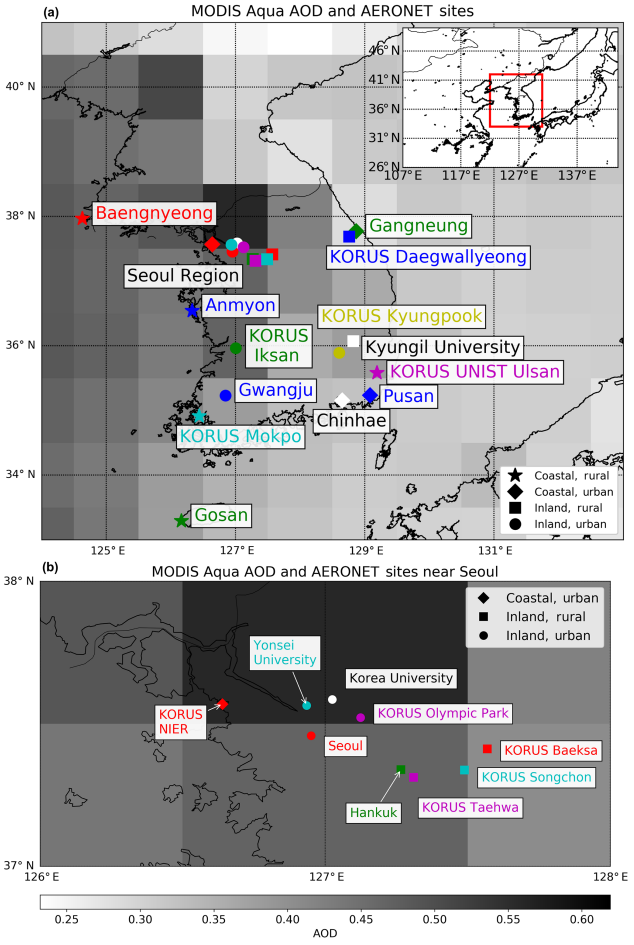

Figure 1. (a) Map of AERONET sites used in this study. The site marker corresponds to its land classification and its color corresponds to Fig. 2. Sites with white markers are not used in Fig. 2 due to their limited data availability. Overlaid is AOD at 550 nm from MODIS Aqua's dark target product. The daily mean data are used. **(b)** Zoom-in of the Seoul region.

3.2 WRF-Chem

The WRF-Chem V3.6.1 model developed by the University of Iowa and NCAR is used. WRF-Chem is a regional meteorology–chemistry model capable of simulating both the chemical and meteorological phenomena within the atmosphere at flexible resolutions to assist with air quality forecasts. It is a fully coupled online model in which both the air quality and meteorological components use the same transport scheme, timestep, grid, and physics schemes for subgrid-scale transport. Additionally, aerosol–radiation–cloud interactions are considered (Grell et al., 2005).

The University of Iowa's WRF-Chem forecast for KORUS-AQ provides simulations of meteorology and atmospheric composition at 20 and 4 km resolution, respectively. A reduced hydrocarbon chemistry mechanism (REDHC) is added to expedite computations, and a simplified secondary organic aerosol formation scheme is added to the sophisticated MOSAIC aerosol module. In the vertical, there are 53 layers distributed between the surface and 50 hPa. The bottom layer closest to the surface has a thickness of $\sim$ 50 m.

To support the KORUS-AQ field campaigns, a Comprehensive Regional Emissions inventory for Atmospheric Transport Experiments (CREATE) was developed based on GAINS-Asia emissions with updated national data (Goldberg et al., 2018). It has 54 fuel classes, 201 sub-sectors, and 13 pollutants, including sulfur dioxide (SO_2), nitrogen oxides (NO_x), carbon monoxide (CO), non-methane volatile organic compounds (NMVOCs), ammonia (NH_3), organic carbon (OC), black carbon (BC), PM_{10}, $PM_{2.5}$, carbon dioxide (CO_2), methane (CH_4), nitrous oxide (N_2O), and mercury (Hg). The emissions of NMVOCs from vegetation are calculated online using the MEGAN (Model of Emis-

Table 1. Details for all 22 AERONET sites. N_{Full} and NKORUS denote the number of observations. N_{Days} denotes the number of days with observations in the full record of data. The hour(s) of AOD minimum and maximum correspond(s) with Fig. 2.

Land classification/site	Full record	N_{Full}	N_{DAYS}	KORUS-AQ record	N_{KORUS}	Hour(s) of AOD minimum (KST)	Hour(s) of AOD maximum (KST)
Coastal, rural							
Anmyon	10/17/99–12/09/15	26 147	1351	–	–	9	18
Baengnyeong	07/25/10–08/31/16	21 113	844	05/01/16–6/13/16	1949	16	7, 18
Gosan	04/04/01–09/12/16	24 208	982	05/01/16–6/14/16	1506	10	16
KORUS Mokpo	03/02/16–01/08/17	7602	196	05/01/16–6/14/16	1728	14	7, 17
KORUS UNIST Ulsan	03/03/16–02/01/17	11 441	231	05/01/16–6/11/16	1989	12	7, 18
Coastal, urban							
Chinhae	04/21/99–09/15/99	796	54			–	–
Gangneung	06/03/12–12/16/15	13 272	569	–	–	11	7, 18
KORUS NIER	02/29/16–06/10/16	1857	80	05/01/16–6/10/16	940	9, 18	8, 13
Pusan	06/16/12–02/11/17	16 253	536	05/01/16–6/11/16	2331	9, 14	7, 18
Inland, rural							
Hankuk	06/01/12–12/21/16	17 341	603	–	–	14	7, 18
KORUS Baeksa	04/24/16–06/14/16	2536	46	05/01/16–6/14/16	2190	12	7, 17
KORUS Daegwallyeong	03/10/16–06/14/16	3152	75	05/01/16–6/14/16	2416	13	10, 16
KORUS Songchon	04/22/16–06/13/16	2576	47	05/01/16–6/13/16	2208	15	9, 18
Kyungil University	11/12/12–12/12/12	617	28		–	–	–
KORUS Taehwa	04/11/16–06/13/16	1939	50	05/01/16–6/13/16	1712	12, 14	8, 17
Inland, urban							
Gwangju	01/04/07–05/20/16	25 531	1,368	05/03/16–5/20/16	3980	14	7, 18
Korea University	06/01/12–07/26/12	1407	34		–	–	–
KORUS Iksan	03/03/16–06/10/16	2725	83	05/01/16–6/10/16	1714	12	7, 17
KORUS Kyungpook	03/02/16–02/14/17	10 443	238	05/01/16–6/14/16	2399	13	7, 18
KORUS Olympic Park	05/01/16–06/14/16	2192	39	05/01/16–6/14/16	2192	14, 18	7, 17
Seoul	02/15/12–07/30/15	8175	382		–	14	7, 18
Yonsei University	03/04/11–01/16/17	65 277	1542	05/01/16–6/13/16	2271	10	7, 18

sions of Gasses and Aerosols from Nature) model, which are influenced by land use, temperature, etc. (Guenther et al., 2006). Biomass burning emissions are taken from the Global Fire Emissions Database (GFED) dataset, which is coupled to a plume-rise model (Grell et al., 2011). Sea salt and dust are calculated using Gong et al. (1997) and Goddard Chemistry Aerosol Radiation and Transport (GOCART; Zhao et al., 2010) schemes, respectively. Chemical initial and boundary conditions are obtained from the Monitoring Atmospheric Composition and Climate (MACC) global tropospheric chemical composition reanalysis.

WRF-Chem data are retrieved according to the latitude and longitude of each of the 15 AERONET sites that were active during the KORUS-AQ timeframe (Table 1). Similar to AERONET, the AOD at 550 nm is calculated. The AOD derived in WRF-Chem is for multiple different observational wavelengths and is based on Ångström exponent relations (Gao et al., 2016; Schuster et al., 2006). The WRF-Chem data are available from 01 May 2016 00:00 UTC to 01 May 2016 11:00 UTC and from 02 May 2016 00:00 UTC to 15 June 2016 23:00 UTC.

3.3 GOCI

The Geostationary Ocean Color Imager (GOCI) onboard the Communication, Ocean, and Metrological Satellites (COMS) is the world's first geostationary ocean color observation satellite. Launched in 2010, it provides spatial coverage of 2500 km × 2500 km in northeast Asia at a 500 m spatial resolution. The domain is comprised of 16 image segments (with resolution of 4 km × 4 km) and the Korean Peninsula sits in the center of it. GOCI has six visible and two near-infrared (NIR) bands at 412, 443, 490, 555, 560, and 680 nm and 745 and 865 nm, respectively (Choi et al., 2012). Observations are taken eight times per day from 00:30 to 07:30 UTC (09:30 to 16:30 KST) (Choi et al., 2017).

To retrieve hourly aerosol data the GOCI Yonsei Aerosol Retrieval (YAER) algorithm was prototyped in 2010 by Lee

et al. (2010) and further developed into its version 1 (V1) form in 2016 by Choi et al. (2016). The aerosol properties from the retrieval include AOD at 550 nm, fine-mode fraction at 550 nm, single-scattering albedo at 440 nm, Ångström exponent between 440 and 860 nm, and aerosol type.

Recently, the V1 algorithm has been enhanced to the version 2 (V2) algorithm and now includes near-real-time (NRT) processing and improved accuracy in cloud masking, determination of surface reflectance, and selection of surface-dependent retrieval schemes. The V2 algorithm (Choi et al., 2018) uses the climatology of land surface reflectance that is obtained from the minimum reflectivity technique; in this technique, the minimum value of multiyear top-of-the-atmosphere reflectances measured by GOCI (for each pixel, each month, and each hour) after Rayleigh correction is considered as the surface reflectance (for that pixel, that month, and that hour). The V2 algorithm has shown similar AOD values at 550 nm to MODIS and the Visible Infrared Imaging Radiometer Suite (VIIRS). When validating with AERONET AOD from 2011 to 2016, the V2 reduced median bias compared to V1, and 62 % and 71 % of the GOCI–AERONET AOD difference is within the expected error (EE) of MODIS dark target (DT) over land and ocean, respectively. For this research, the GOCI YAER V2 AOD at 550 nm data are downloaded for the KORUS-AQ campaign from 1 May 2016 to 12 June 2016.

3.4 $PM_{2.5}$

$PM_{2.5}$ data are downloaded from the KORUS-AQ data repository for the entirety of the field campaign. The 10 sites with a corresponding AERONET site nearby are used for this research (Table 2). The three sites of Busan, Gwangju, and Seoul have multiple sensors within the city limits; thus, their total number of observations during the KORUS-AQ timeframe is much larger than the other seven sites. Additionally, the Hankuk University of Foreign Studies (HUFS) site records data every minute while the others take hourly measurements. All four land classifications are represented within the group, although there is only one inland rural site. All data during the KORUS-AQ timeframe are downloaded and the number of days with data ranges from 35 to 41. Overall, there are 51 monitors from Air Korea, 6 from the National Institute of Environmental Research (NIER), 1 from the Seoul Research Institute on Public Health and Environment (SIHE), and 1 from the HUFS. It should be noted that 51 of the 59 data files had quality control techniques applied to them at the date of last access in August 2017.

4 Methods and analysis

4.1 Analysis of AOD diurnal variation

The AOD at each hour is computed by using instantaneous AERONET AOD measurements within ±30 min centered over that hour. The hourly AOD for the same hour in different days is then averaged to compute the climatological AOD for that hour; the baseline AOD for each hour is then used to compute baseline daily-mean AOD, from which the diurnal variation of AOD values for each hour can be subsequently calculated. This is completed for the hours of 00:00–10:00 and 21:00–23:00 UTC due to the conversion to Korea Standard Time. KST is 9 h ahead of UTC, so the diurnal variation period extends from 07:00 to 18:00 KST, as the first and last hour are excluded for a lack of observations.

Furthermore, to calculate the statistics for hourly variations, the percent difference from the (baseline) daily mean is computed. This is referred to as the percent departure from average. Our methods here are similar to the methods from Wang et al. (2004) and Smirnov et al. (2002). Hence, expressing the departure as a percent allows for comparison to other AOD studies.

The original 22 AERONET sites are split into four land classifications to further analyze and define trends amongst their AOD diurnal variations at 550 nm. The sites of Chinhae, Korea University, and Kyungil University are excluded from the analysis due to the short data records, leaving 19 AERONET sites. Each site's full record of data is used in the calculation (Table 1). Figure 1 shows a summary of this classification. Of the 19 sites, 3 are coastal urban, 5 are coastal rural, 6 are inland urban, and 5 are inland rural.

Shown in Fig. 2 is the AOD diurnal variation and percent departure from daily mean using the full record of data at all 19 AERONET sites, split into land classification. The coastal rural sites show the most similarity amongst each other and are characterized by AOD levels remaining virtually constant throughout the day as their departure from the daily mean is generally ±10 %. This feature agrees with Smirnov et al. (2002), who also found that the Anmyon site, on the western coast of the Korean Peninsula, has little to no diurnal variation of AOD at 500 nm when investigating a multiyear data record.

The AOD diurnal variation of the coastal urban sites is more pronounced with a departure from the daily average at ±20 % and has fewer intra-class similarities as compared to the costal rural class. The KORUS NIER site has noticeably higher values of AOD than the Gangneung or Pusan sites for the majority of the day until 18:00 KST. These sites are urban in nature and therefore have their own emissions characteristics, adding an additional layer of complexity to their distinctive diurnal variations. This could explain why the coastal urban sites experience more variation than the coastal rural sites. When focusing on the different diurnal variations amongst the coastal urban sites, we believe that

Table 2. The 10 KORUS-AQ ground sites with $PM_{2.5}$ data and their corresponding AERONET station.

Land classification/ $PM_{2.5}$ site	Full record	N_{Full}	AERONET site	N_{DAYS}	Hour(s) of $PM_{2.5}$ minimum (KST)	Hour(s) of $PM_{2.5}$ maximum (KST)
Coastal, rural						
Baengnyeong	05/08/16–06/12/16	825	Baengnyeong	36	7, 18	14
Jeju	05/08/16–06/12/16	632	Gosan	35	10, 13	11, 14
Ulsan	05/09/16–06/12/16	840	KORUS UNIST Ulsan	35	11	18
Coastal, urban						
Bulkwang	05/08/16–06/12/16	839	KORUS NIER	36	13	8
Busan (19)	04/29/16–06/10/16[a]	19 192	Pusan	41	10	17
Inland, rural HUFS	05/08/16–06/12/16	48 183[b]	KORUS Songchon	36	18	8
Inland, urban						
Daejeon	05/08/16–06/12/16	841	KORUS Iksan	36	15	8
Gwangju (7)	04/29/16–06/10/16[a]	6794	Gwangju	41	7	17
Olympic Park	05/09/16–06/17/16[c]	917	KORUS Olympic Park	38	15, 18	8, 17
Seoul (26)	04/29/16–06/10/16[a]	26 095	Yonsei University	41	16	10

[a] means that only data from 5/1/16–6/10/16 are used. [b] means that the data are for every minute versus the other data that are hourly, hence the large number of observations. [c] similarly means that only data from 5/9/16–6/15/16 are used since the KORUS-AQ timeframe is defined in this study as 5/1/16–6/15/16. Sites with a number in parenthesis denote how many individual stations were within that city, contributing to the higher number of observations.

the differences could stem from the site location. For example, the sites on the western Korean Peninsula (i.e., KORUS NIER) are closer to Chinese emissions and may be impacted more by long-range transport than the coastal urban sites on the eastern Korean Peninsula (i.e., Pusan and Gangneung). When combined with local emissions, the external factors could lead to a different diurnal variation than their counterparts on the eastern side of the country.

All six of the inland urban sites show remarkably similar diurnal variations. Their AODs slightly decrease and remain constant until the early afternoon at approximately 14:00 KST when the AOD then gradually builds until 18:00 KST. One outlier to this late afternoon building characteristic is KORUS Olympic Park, whose AOD values drop between 17:00 and 18:00 KST. As a whole, their average departure from the daily mean is ± 20 %, with the most negative values occurring in the midday (i.e, the inland urban sites experience minima in AOD values during this time). The early morning and late evening increases could be attributed to an increase in traffic and transportation demands. It is interesting to note that this common diurnal variation trend is seen at sites that have as little as 4 months of data (i.e., KORUS Iksan) to more than 5 years of data (i.e., Gwangju and Yonsei University). Below in Sect. 4.3, we investigate this further to quantify how long of a record is needed at each site to match the diurnal variation produced by the full record.

The five inland rural sites naturally divide into two groups. KORUS Daegwallyeong, located on the eastern part of the peninsula, shows a much lower magnitude of AOD around 0.2–0.3 throughout the entire day. The other four locations of Hankuk, KORUS Baeksa, KORUS Songchon, and KORUS Taehwa have higher AOD values near 0.4–0.6 in the morning before decreasing throughout the day and eventually rising again in the early evening at 15:00–16:00 KST. The only two exceptions to this trend are Hankuk and KORUS Songchon, located east-southeast of Seoul, which experience slight noontime increases. After the late afternoon buildup, most of the sites' AOD decreases at 17:00–18:00 KST, again with the exception of Hankuk and KORUS Songchon. The inland rural sites have the most variation for their percent departure from average with some sites such as KORUS Baeksa and KORUS Songchon approaching -30 % at 12:00 and 15:00 KST, respectively, and KORUS Daegwallyeong staying between ± 10 % with the exception of 16:00 and 17:00 KST.

Overall, we see similar trends for the coastal sites and for the inland sites. The coastal urban and coastal rural sites have a lower average AOD value of 0.308 compared to the inland urban and inland rural sites whose average AOD value is 0.386. Additionally, regardless of land classification, most sites see early morning and late afternoon AOD maxima and noontime AOD minima. Factors influencing the diurnal variation include length of the data record, number of available measurements for calculating the hourly averages, and site location compared to those sharing its land classification.

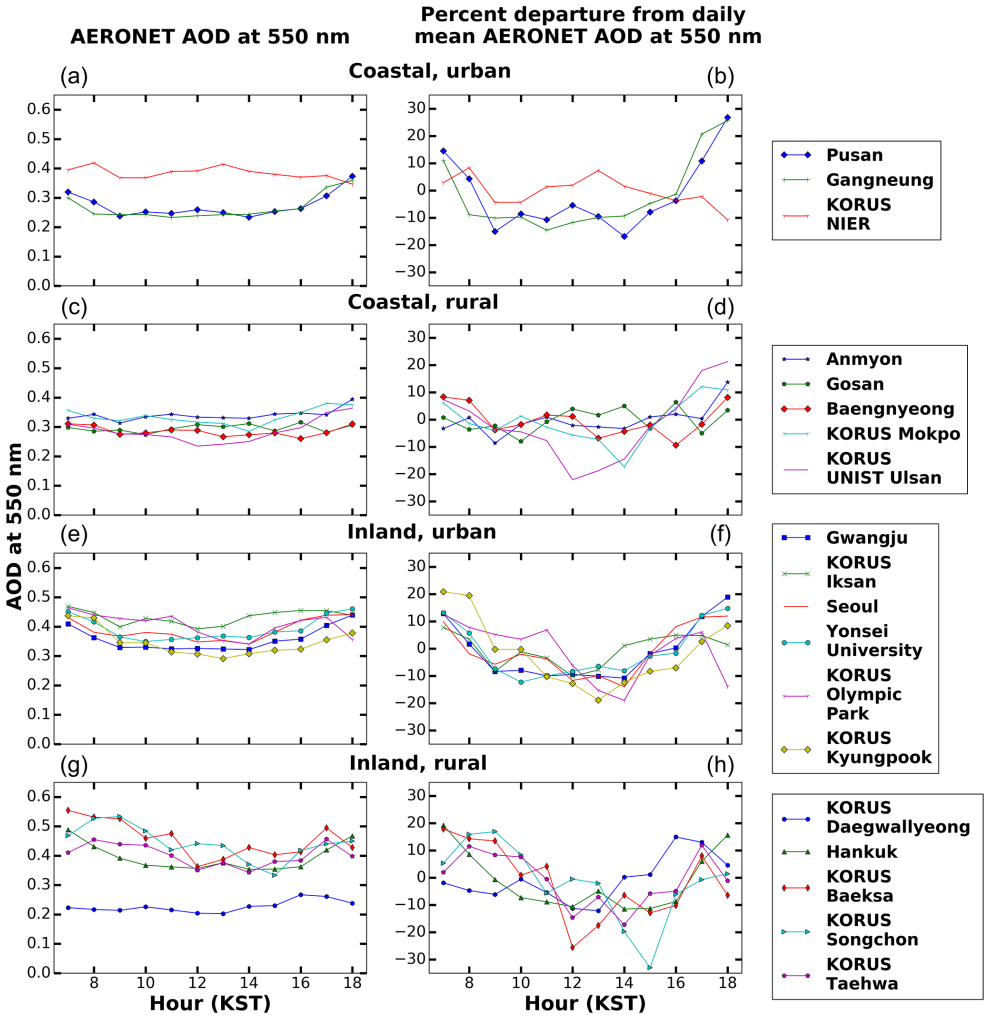

Figure 2. The AOD diurnal variation and percent departure from daily mean using the full record of AERONET AOD at 550 nm data for the 19 sites of interest.

4.2 Analysis of the Ångström exponent diurnal variation

Similar to the AOD diurnal variation, each site's full record of data is used to compute the diurnal variation of the Ångström exponent. The same analysis procedure is used, but, instead of calculating AOD at 550 nm, the only variable of interest is the Ångström exponent between 440 and 675 nm. The Ångström exponent is of importance since it helps determine the aerosol's source. It is inversely related to the average size of aerosol particles, so the smaller the particles, the larger the value. Generally speaking, an Ångström exponent approaching 0 signifies coarse-mode or larger particles such as dust, and an Ångström exponent greater than or approaching 2 signifies fine-mode or smaller particles such as smoke from biomass burning and anthropogenic aerosols (Wang et al., 2004). The size of the particle assists with attributing the aerosol to natural or anthropogenic sources since the latter are typically smaller than their natural counterparts (of dust and sea salt particles); this is especially true for the KORUS-AQ because biomass burning sources in east Asia in the growing season (e.g., the study period here) are minimal (Polivka et al., 2015).

All four land classifications show similar Ångström exponent values in the range of 1.2–1.6 with the exception of lower values near 1.0 at the inland rural sites (Fig. 3). All six of the inland urban sites experience a gradual increase in the Ångström exponent from 1.2 to 1.4 throughout the day. The coastal urban sites are similar, as Pusan and Gangneung also see an increase in the Ångström exponent, but the KORUS NIER site has a noticeable Ångström exponent maximum near 1.2 at 10:00 KST. Also, its values are lower than the other coastal urban or inland urban sites, with a range of 1.1 to 1.2. However, the general trend of the coastal urban sites is that they too gradually increase in Ångström exponent as the day progresses.

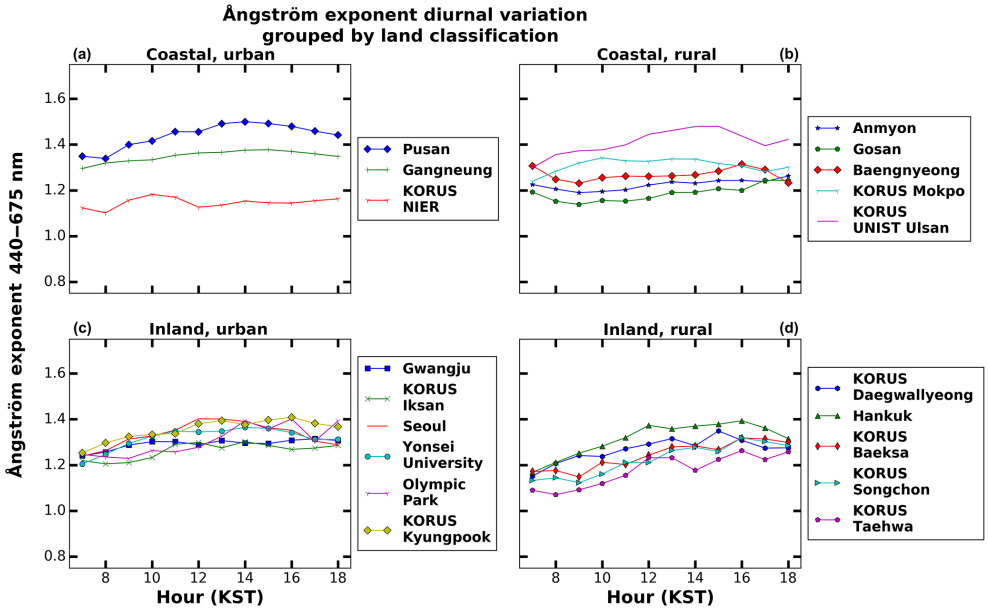

Figure 3. The Ångström exponent 440–675 nm diurnal variation using the full record of AERONET data for the 19 sites of interest.

Turning to the rural sites, all five of the inland rural sites experience the same gradual rise throughout the day to 1.4 as the inland urban sites, but their values start a bit lower near 1.0 versus 1.2. The coastal rural sites hover ~ 1.3 for the majority of the day, with KORUS UNIST Ulsan experiencing values as high as 1.5 from 12:00 to 16:00 KST before dropping back down to 1.4 by 17:00 KST. The Ångström exponent diurnal variation of the coastal rural sites is not as pronounced as that in the other three land classifications that all experience morning Ångström exponent minimums and gradually build throughout the day before plateauing.

With the typical range of 1.2–1.6 experienced at most sites, it is concluded that the majority of aerosols over the Korean Peninsula are fine-mode particles with some coarser-mode particles seen overnight and in the early morning. As the day progresses, the particle size decreases due to secondary organic aerosol formation which leads to an increase in the Ångström exponent.

4.3 Observation time for climatologically representative AOD diurnal variation

In this section, we define the term "climatological diurnal variation". This is the diurnal variation pattern produced at each AERONET site in long-term averages such that it is relatively persistent and statistically robust. The concept is similar to the concept of climatology of diurnal variation of 2 m air temperature which, while varying with location, normally shows a peak in the afternoon and minimum before the sunrise (Wang and Christopher, 2006; Aegerter et a., 2017). The concept of climatological diurnal variation of AOD or aerosol properties, therefore, builds upon the hypothesis that there are underlying processes inherent with respect to a specific location to produce diurnal variation of AOD. For example, in the agricultural burning seasons over Central America, AOD values often peak around late afternoon and are minimal in the night before the Sun rises; this is because such burnings often start in the late morning and diminish at night (Wang et al., 2006). Hence, an intriguing question is how long our data record should be to obtain the climatological diurnal variation of AOD or aerosol properties. We address this question by data collected at the five AERONET sites which have more than 5 years of data in their full record: Anmyon, Baengnyeong, Gosan, Gwangju, and Yonsei University.

To statistically compare how long of a data record is needed to match the climatological diurnal variation, we first compute the statistics starting from the first month of the data record to a certain number of months, n; hereafter, the subset of the data is denoted as $[1, n]$, with the first number being the starting month and the second number the last month in the subset. We then repeat the calculation by moving the starting month (and ending month) with an increment of 1 month each time, e.g., for the data subset $[2, n+1]$, $[3, n+2]$, $\ldots$, $[N-n+1, N]$, where N is the total number of months of the whole data record. The average of diurnal variation statistics from each n-month data subset is then compared with statistics of diurnal variation from the whole data record. The comparison reveals the degree to which the n-month data record may describe the climatological diurnal variation derived from the full data record for a specific site of interest. We then repeat the same process by increasing the number of months for the subset (n) by 1 month, 2 months, 3 months, etc., until the subset eventually grows to the full

record. It is expected that as n increases, the climatological diurnal variation will be better characterized.

The actual implementation of the method above requires the removal of the gaps of missing data, e.g., months that don not have observation. Hence, Anmyon, Baengnyeong, Gosan, Gwangju, and Yonsei University are left with full records of 89, 53, 80, 82, and 71 months, respectively, for the analysis.

Figure 4 shows that as n, the number of months of observation, increases, the diurnal variation being described by these subset observations is in more agreement with the counterpart from the full record, in terms of the linear correlation coefficient R, root mean square error (RMSE), and statistical significance. The inland urban sites of Gwangju and Yonsei University have very similar results (Fig. 4d and e). Gwangju requires 13 months of data to become significant ($p < 0.05$), or roughly 15.9 % of the full (82 months) record of data. Yonsei requires 11 months of data, which is slightly lower at 15.5 % of the record (of 71 months). Additionally, they both have an R value around 0.8 at the occurrence of the first significance, and their results become significant shortly after the RMSE and R-value graphs intersect. We conclude that the inland urban sites require 10–12 months of data to match the climatological diurnal variation with an R value of 0.8 and $p < 0.05$. Additionally, they require 45–47 months of data for an RMSE <0.02.

The results for coastal rural sites of Anmyon, Baengnyeong, and Gosan are less cohesive (Fig. 4a–c). They require more data than the urban sites before becoming significant ($p < 0.05$), with a range from 18 % to 32 %. Anmyon requires 16 of the 89 months (16/89) or 18 % of the total data, and Baengnyeong and Gosan require about 30 % of the total data (17/53 and 24/80 months, respectively). They have slightly lower R values of 0.57–0.78 at the time of their first significance, and, similar to the inland urban sites, their correlations become significant after the intersection of the RMSE and R-value graphs. These three sites require 21–25 months of data to match their climatological diurnal variations with an R value of 0.8 and $p < 0.05$, which is twice that of the inland urban sites. Overall, RMSE < 0.02 can be reached with 35–52 months of data in the subset; this is similar to the inland urban sites, but at a much greater range. The varied location of these three coastal rural sites could explain the variability between them, as they extend from Baengnyeong near North Korea to Gosan off the southern coast of the Korean Peninsula.

Between the five sites that we investigated, there is no consistent pattern amongst the number of months of full record data required for diurnal variation replicability and significance. Baengnyeong, the site with the shortest full data record (53 months), requires 16 months (32 %) of the data, while Yonsei (71 months of data) requires 11 months (15.5 %), Gosan 24 months, Gwangju 13 month, and Anmyon 16 months. On average, $\sim$ 18 months of observation data are needed to obtain statistically significant results for characterizing the diurnal variation of AOD.

One surprising finding, which is interesting to note, is that coastal rural sites would require a record twice as long as that of the inland urban sites to match the climatological diurnal variation with $R = 0.8$ and $p < 0.05$. We thought that, due to the complexity of the urban sites having both their own emissions and those via background and transport, they would require more data for a common trend to emerge. However, it is in fact just the opposite, suggesting that the diurnal variation of AOD in an urban setting is distinct and persistent.

4.4 Analysis of WRF-Chem and GOCI AOD

The WRF-Chem model provided hourly chemical weather forecasts from 1 May to 15 June 2016. Thus, this is defined as the KORUS-AQ timeframe, and spatial and temporally matched data pairs between GOCI–AERONET and WRF-Chem–AERONET are analyzed. GOCI AOD data are rarely captured eight times per day due to clouds, and the AERONET data undergo their own quality control algorithms to ensure cloud-free conditions. In contrast, the WRF-Chem data are available for every hour during the timeframe of interest. Due to these factors, the intercomparison dataset is the smallest between AERONET vs. GOCI (1583 data pairs) and the largest between AERONET vs. WRF-Chem (3633 data pairs).

The scatter plots between observation (x axis) and either model or GOCI (y axis) are shown in Fig. 5. Although both are statistically significant ($p < 0.001$), the AERONET vs. GOCI R value of 0.8 is double that of the AERONET vs. WRF-Chem R value of 0.4. Additionally, the RMSE value for AERONET vs. GOCI is lower as well. Overall, WRF-Chem can both over- and underpredict the AERONET AOD values, thereby yielding no bias overall, while the GOCI satellite typically underpredicted them during the KORUS-AQ timeframe (with an overall low bias of 0.04). Because of this systematic low bias, only $\sim$ 40 % of GOCI–AERONET AOD difference is within EE of MODIS DT over land, and this 40 % can be increased to 56 % after accounting for this bias (Fig. 5c). Also, because of no obvious bias in WRF-Chem AOD, $\sim$ 46 % of the WRF-Chem vs. AERONET AOD difference is within EE of MODIS AOD over land, which is slightly higher than the counterpart for GOCI vs. AERONET. In reference to the AERONET AOD values, GOCI AOD has smaller RMSE (0.16) than that (0.28) of WRF-Chem predictions.

To analyze these results on a site basis, Taylor diagrams are produced (Fig. 6), in which the radius represents the normalized standard deviation while the correlation coefficient is represented as the cosine of the polar angle. Hence, regardless of the data sources, the observation data will be represented at the one point (with a normalized standard deviation of 1 and a cosine of the polar angle of 1). The color of data points shows the data bias with respect to the observation.

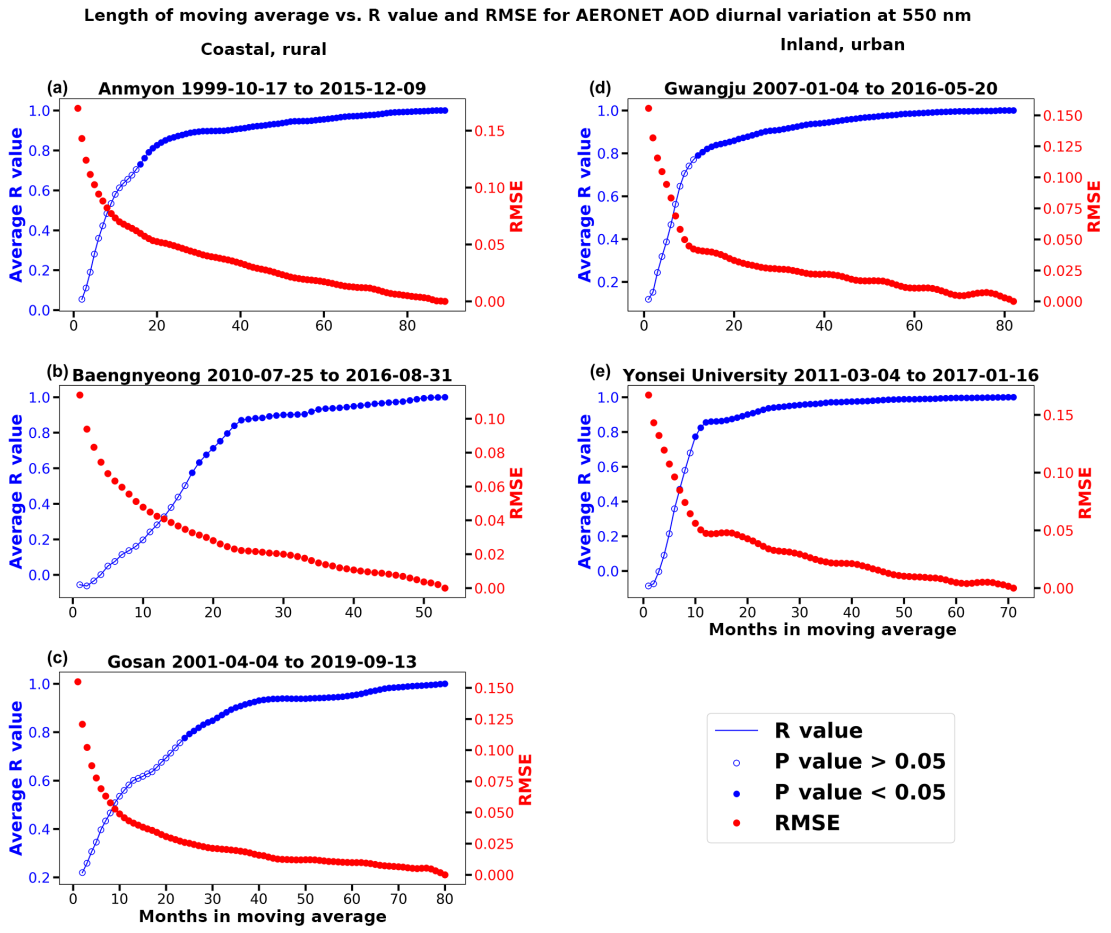

Figure 4. Establishing how long of a record of data is needed to match the climatological AOD at 550 nm diurnal variation. Anmyon, Baengnyeong, and Gosan are all coastal, rural sites. Gwangju and Yonsei University are inland, urban sites. The R value 5 is in blue, the RMSE value is in red, and the p value corresponds to the marker characteristic. A filled-in marker represents $p < 0.05$ and an open marker represents $p > 0.05$.

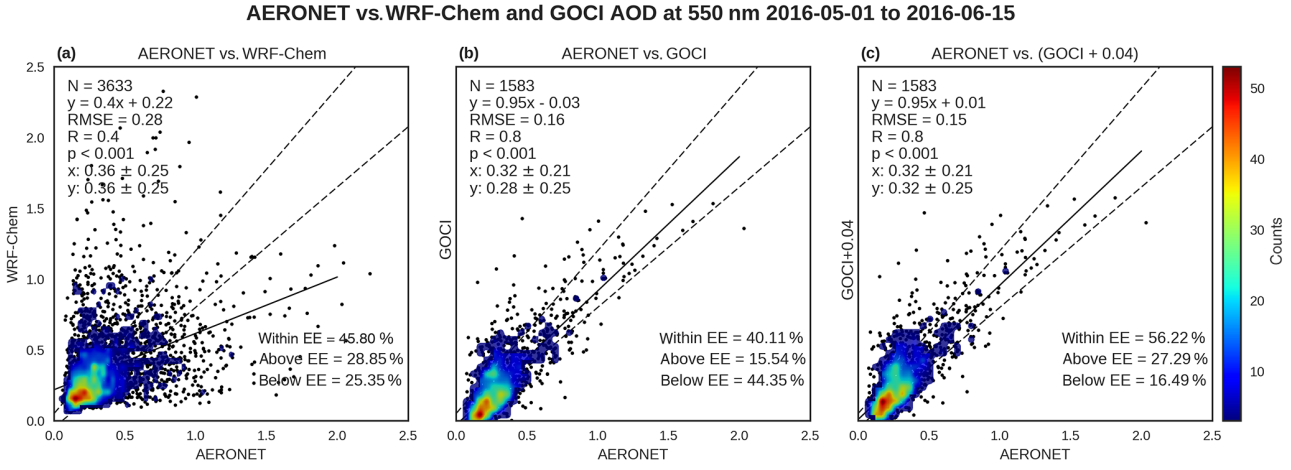

Figure 5. AERONET vs. WRF-Chem **(a)** and AERONET vs. GOCI AOD **(b)** at 550 nm for the KORUS-AQ Campaign from 1 May to 15 June 2016. Only the temporally and spatially matched data are used. The point color corresponds to the number of observations within that area. Also shown is the AERONET vs. GOCI AOD after the latter is added by 0.04 **(c)**.

Figure 6a shows that WRF-Chem both over- and underpredicted AOD values during the campaign, and there is no clear indication that the WRF-Chem performed consistently better for certain land classification (within the 15 sites we analyzed). For example, looking at the inland urban sites, WRF-Chem underpredicted two sites (KORUS Olympic Park and KORUS Iksan), overpredicted two sites (Gwangju and KORUS Kyungpook), and had no bias at one site (Yonsei University). The R values range from 0.15 to 0.7 with the majority of points between 0.15 and 0.4. Lastly, there is an even distribution of sites where the WRF-Chem standard deviation is higher than or less than the AERONET standard deviation.

Figure 6b shows the relationship between AERONET and GOCI at the same 15 sites during the KORUS-AQ campaign. Here, we see that only three sites (Baengnyeong, KORUS NIER, and KORUS Daegwallyeong) had a positive bias and thus were overestimated by GOCI. Noticeably different from Fig. 6a is the shifted R-value range, now extending from 0.35 to 0.9 but concentrated within 0.7 to 0.9. Another interesting difference is that the GOCI standard deviation was greater than the AERONET standard deviation at all 15 sites, suggesting GOCI AOD tends to amplify the temporal variation of AOD and could be attributed to larger random errors than AERONET AOD.

4.5 $PM_{2.5}$ diurnal variation

Table 2 lists information for all $PM_{2.5}$ sites, including their full record of data, the number of recorded observations within that full record, the nearby AERONET station, the number of days having data recorded, and the hours of minima and maxima for $PM_{2.5}$. A total of 9 of the 10 sites reported data in hourly averages. For the HUFS site whose data were reported every minute, the hourly averages are created by computing the mean of the data in that hour, as is done by most analyses of hourly $PM_{2.5}$. Again, only 07:00–18:00 KST is analyzed for $PM_{2.5}$.

As seen in Fig. 7, the $PM_{2.5}$ diurnal variations are surprisingly invariant given the short timeframe of interest (the 6-week KORUS-AQ field campaign). One would expect that, as the data timeframe decreases, the fluctuations would increase. However, this is not the case for $PM_{2.5}$. The coastal urban sites of Busan and Bulkwang remain near 30–35 $\mu g\,m^{-3}$ throughout the day (Fig. 7a). Bulkwang does slightly increase at 08:00 KST but then returns to the constant value of 30 $\mu g\,m^{-3}$ by 11:00 KST. The inland urban sites (Fig. 7b) closely resemble the coastal urban sites in diurnal pattern and value except for Olympic Park. Its values were double the other inland and coastal urban sites at 60 $\mu g\,m^{-3}$ at its 08:00 KST maximum. Concentrations then drop to near 45 $\mu g\,m^{-3}$ for 13:00–18:00 KST. Olympic Park shows the most fluctuations throughout the day in its $PM_{2.5}$ concentrations.

The coastal rural sites (Fig. 7c) of Jeju, Baengnyeong, and KORUS UNIST Ulsan split into three diurnal variations that

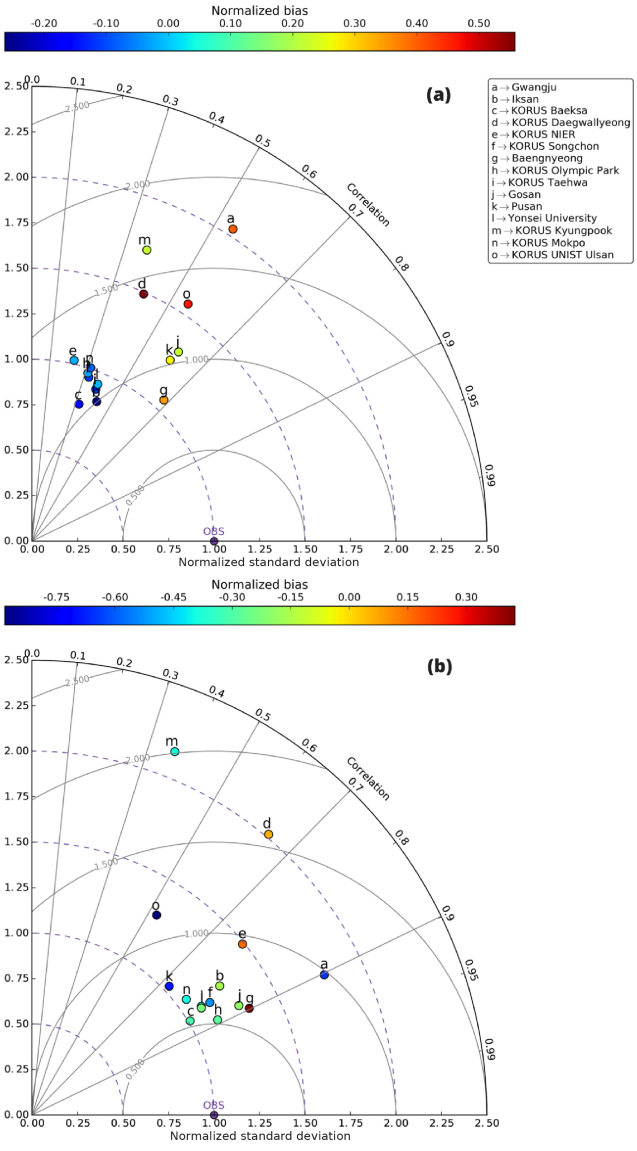

Figure 6. Taylor diagrams of **(a)** AERONET AOD vs. WRF-Chem AOD and **(b)** AERONET AOD vs. GOCI AOD.

are varied in concentration and each with its own unique pattern. The KORUS UNIST Ulsan site has the highest concentrations near 30 $\mu g\,m^{-3}$ but exhibits little to no fluctuations throughout the day. The Baengnyeong site has the second highest concentrations near 25 $\mu g\,m^{-3}$ with a 14:00 KST maximum. Jeju has the lowest concentrations near 15 $\mu g\,m^{-3}$ on average, with maxima at 11:00 and 14:00 KST and with minima at 10:00 and 13:00 KST; the difference between maxima and minima is within 4 $\mu g\,m^{-3}$ (or $\sim$ 10–12 % from the mean), suggesting an insignificant pattern for diurnal variation. HUFS, the inland rural site (Fig. 7d), fluctuates between its 08:00 KST maxima near 40 $\mu g\,m^{-3}$ and drops to a concentration near 30 $\mu g\,m^{-3}$ by 12:00 KST and remains there for the rest of the day.

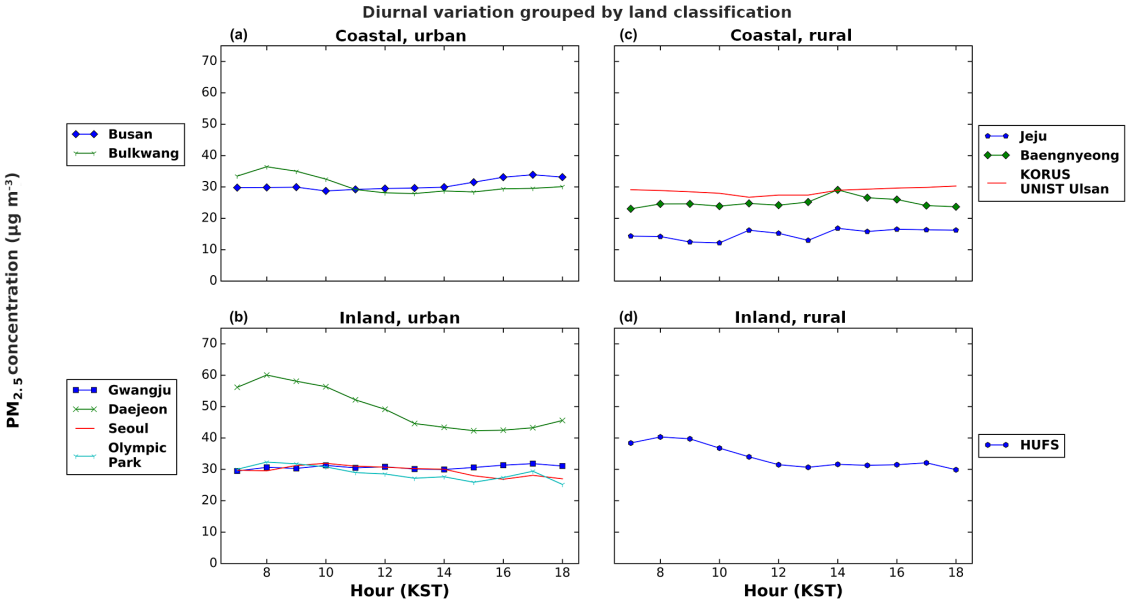

Figure 7. The $PM_{2.5}$ diurnal variation using the 10 KORUS-AQ ground sites that have a corresponding AERONET station nearby. The 24 h $PM_{2.5}$ air quality standard in South Korea is 50 mg m^{-3} and the WHO recommendation is 25 mg m^{-3}.

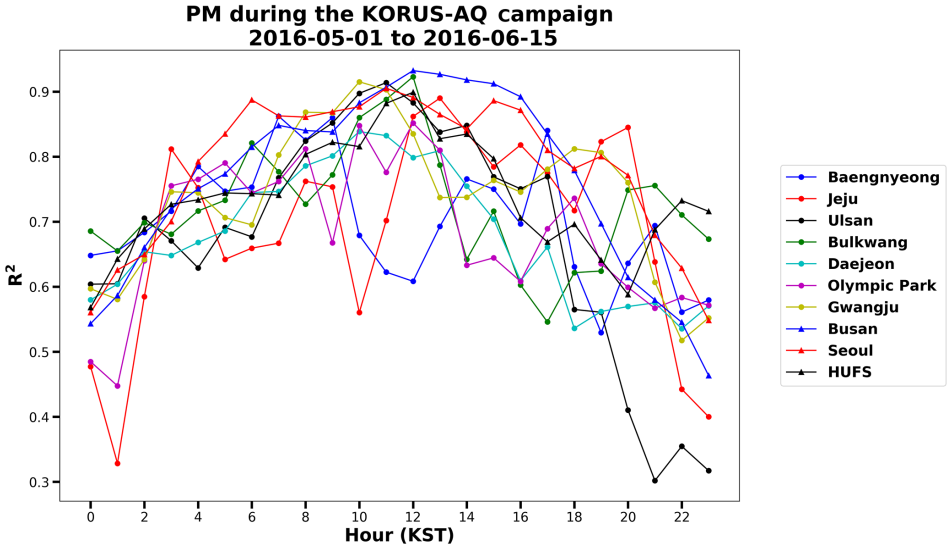

Figure 8. The diurnal variation of R^2 for $PM_{2.5}$ for the sites in Table 2.

Overall, Fig. 7 shows $PM_{2.5}$ values generally have dual peaks, with the strongest peak in the morning hours (08:00–10:00 KST) and a weak peak in the early afternoon hours (around 14:00 KST). However, such a pattern does vary by station and can be insignificant in most sites. A total of 7 of the 10 sites have stagnant $PM_{2.5}$ values near 30 µg m^{-3} throughout the entire day. The other three sites, Bulkwang, Daejeon, and HUFS, all have morning $PM_{2.5}$ maxima at 08:00 KST before dropping to stagnant values by 13:00 KST. Daejeon experiences abnormally high $PM_{2.5}$ concentrations with values peaking near 60 µg m^{-3}. For all sites, the correlation between hourly $PM_{2.5}$ variation and daily-mean $PM_{2.5}$ variation (Fig. 8) has the highest R^2 value above 0.8 at noontime, decreases toward early morning and late afternoon, and reaches the minimum at midnight, which suggests that daytime variation of emission and boundary layer processes are the dominant factors affecting day-to-day variability of $PM_{2.5}$.

4.6 The AOD–$PM_{2.5}$ diurnal variation relationship

Here we study which data source (from GOCI or WRF-Chem) either predicted or retrieved the AERONET AOD values better. We also compare the AOD diurnal variation to the $PM_{2.5}$ diurnal variation. In Fig. 9, the diurnal variations are shown for AERONET, WRF-Chem, GOCI, observed $PM_{2.5}$, and WRF-Chem-predicted $PM_{2.5}$ for the sites that have all five dataset available (i.e., the sites listed in Table 2). All data are temporally and spatially matched. Due to its retrieval times, GOCI's AOD diurnal variation only extends from 09:00 to 16:00 KST, thus only 09:00–16:00 KST is used for AERONET and WRF-Chem as well.

The GOCI AOD values better matched the observed AERONET AOD diurnal variation. As seen in Fig. 9a, although hourly GOCI AOD has a systematic low bias of 0.04–0.09 with respect to the AERONET counterparts, the GOCI AOD diurnal variation (green line) mirrors that of AERONET (blue line) for the entire day, showing low values around noon and dual peaks (one in 10:00–11:00 KST) in the morning and (another 14:00 KST) in the afternoon, respectively; both GOCI and AERONET show that the minimum AOD is in the late afternoon at 16:00 KST, although GOCI shows a relatively larger decrease in AOD from 14:00 to 16:00 KST. In contrast, while WRF-Chem AOD values are consistent with GOCI and AERONET to describe the dual peaks and low AOD values around noon, a much stronger peak at 16:00 KST (than that at 10:00 KST) in WRF-Chem differs from GOCI and AERONET (both of which show comparable dual peaks). Furthermore, WRF-Chem shows a relative increase in (minimum) AOD at 09:00–15:00 and 16:00 KST, while GOCI and AERONET both show the decrease with minimum AOD at 16:00 KST. Hence, it is hypothesized that the diurnal emission in WRF-Chem may have an overly strong tendency toward afternoon emission; indeed WRF-Chem AOD is comparable to AERONET AOD values in the morning, but shows a large positive bias up to 0.08 in the late afternoon. This hypothesis needs to be further studied.

Also plotted in Fig. 9a is the average observed and WRF-Chem-predicted $PM_{2.5}$ diurnal variation of the 10 $PM_{2.5}$ sites. The observed concentrations peak at 10:00 KST with a value approaching $33\,\mu g\,m^{-3}$, but drop to less than $28\,\mu g\,m^{-3}$ by 13:00 KST, and then peak again to $30\,\mu g\,m^{-3}$ at 14:00 KST. The WRF-Chem-predicted $PM_{2.5}$ is systematically higher than observed $PM_{2.5}$ by 10–$15\,\mu g\,m^{-3}$, but it has similar dual peaks at 10 and 14:00 KST. Similar to AOD, WRF Chem showed that the peak at 14:00 KST is $\sim 3\,\mu g\,m^{-3}$ higher than the peak at 10:00 KST, while observed $PM_{2.5}$ data show that the peak at 14:00 KST is $\sim 5\,\mu g\,m^{-3}$ lower than the peak at 10:00 KST. Furthermore, WRF-Chem shows an increase in $PM_{2.5}$ from 11:00 to 13:00 KST while the observed $PM_{2.5}$ showed the opposite. Overall, the observed $PM_{2.5}$ concentrations decrease from morning (09:00–10:00 KST) to evening (15:00–16:00 KST), but WRF-Chem counterparts show the opposite. Hence, the comparison and contrast analyses of both AOD and $PM_{2.5}$ suggest further studies for the diurnal variation of emissions in WRF-Chem.

In general, the diurnal variation of AERONET AOD (averaged over all sites) fluctuates the least throughout the day with a percent departure from the daily mean of $\pm 6\,\%$. WRF-Chem fluctuates $\pm 8\,\%$ while GOCI shows the most variation at $+9\,\%$ to $-30\,\%$ due to an outlying low value at 16:00 KST. Similar to AERONET and WRF-Chem, the $PM_{2.5}$ percent departure from daily mean ranges from $\pm 8\,\%$.

Figure 9b displays the diurnal variation of the $PM_{2.5}$ / AOD ratio derived from WRF-Chem and collocated AERONET AOD vs. in situ $PM_{2.5}$ ratio and GOCI AOD vs. in situ $PM_{2.5}$ ratio measurement throughout the KORUS-AQ campaign. The comparison of the $PM_{2.5}$ / AOD ratio is valuable because satellite AOD often is used to multiply this ratio to derive surface $PM_{2.5}$. Overall, the WRF-Chem $PM_{2.5}$ / AOD ratio (with a mean of $154\,\mu g\,m^{-3}\tau^{-1}$) is 30 %–50 % larger than and shows temporal disparity with the observed counterparts (with a mean of 110 and $103\,\mu g\,m^{-3}\tau^{-1}$, respectively); it shows a steady decrease from morning to the late afternoon, while the observation-based ratios (based on GOCI or AERONET AOD vs. in situ $PM_{2.5}$) are consistent with each other in terms of mean (with correlation of 0.63, Fig. 9b) – they first decrease in the morning, reach the minimum in the late morning (11:00 KST), and then increase steadily toward the late afternoon. However, there is no apparent trend between the $PM_{2.5}$ / AOD ratio and time of day at individual sites (Fig. 10). Additionally, the correlation between the WRF-Chem ratio and the observed ratio (Fig. 10) can vary from 0.28 to 0.78, depending on the specific location of each site (Fig. 10). Except Daejeon for some hours and one outlier at a particular hour in the Gwangju site (Fig. 10), all other sites show that WRF-Chem's $PM_{2.5}$ / AOD ratio is larger than observation-based counterparts, with the majority of the ratios ranging from 60 to $140\,\mu g\,m^{-3}\tau^{-1}$ with outliers as low as 40 and as high as $160\,\mu g\,m^{-3}\tau^{-1}$ (Fig. 10). The three coastal rural sites of Baengnyeong, Jeju, and Ulsan have ratio maximums both in the morning (07:00, 08:00, and 10:00 KST) and early evening (17:00 KST). Their minimums range from morning (09:00 KST) to noontime and late afternoon (16:00 KST). The two coastal urban sites of Bulkwang and Busan show more similarities with peaks in the early morning (08:00 and 09:00 KST) but still have a minimum range from noontime to afternoon (12:00 and 15:00 KST). The inland urban sites have morning (09:00 and 10:00 KST), afternoon (13:00 KST), and early evening (17:00 and 18:00 KST) maximums but cohesively have a 15:00 KST minimum, aside from Gwangju whose ratio steadily increases after 10:00 KST. Being the only inland rural site, the $PM_{2.5}$ / AOD at HUFS has maxima at 08:00 KST and steadily decreases afterward for the remainder of the day. Consequently, given the large spatial and temporal variations of the $PM_{2.5}$ / AOD ratio, diurnal variation of

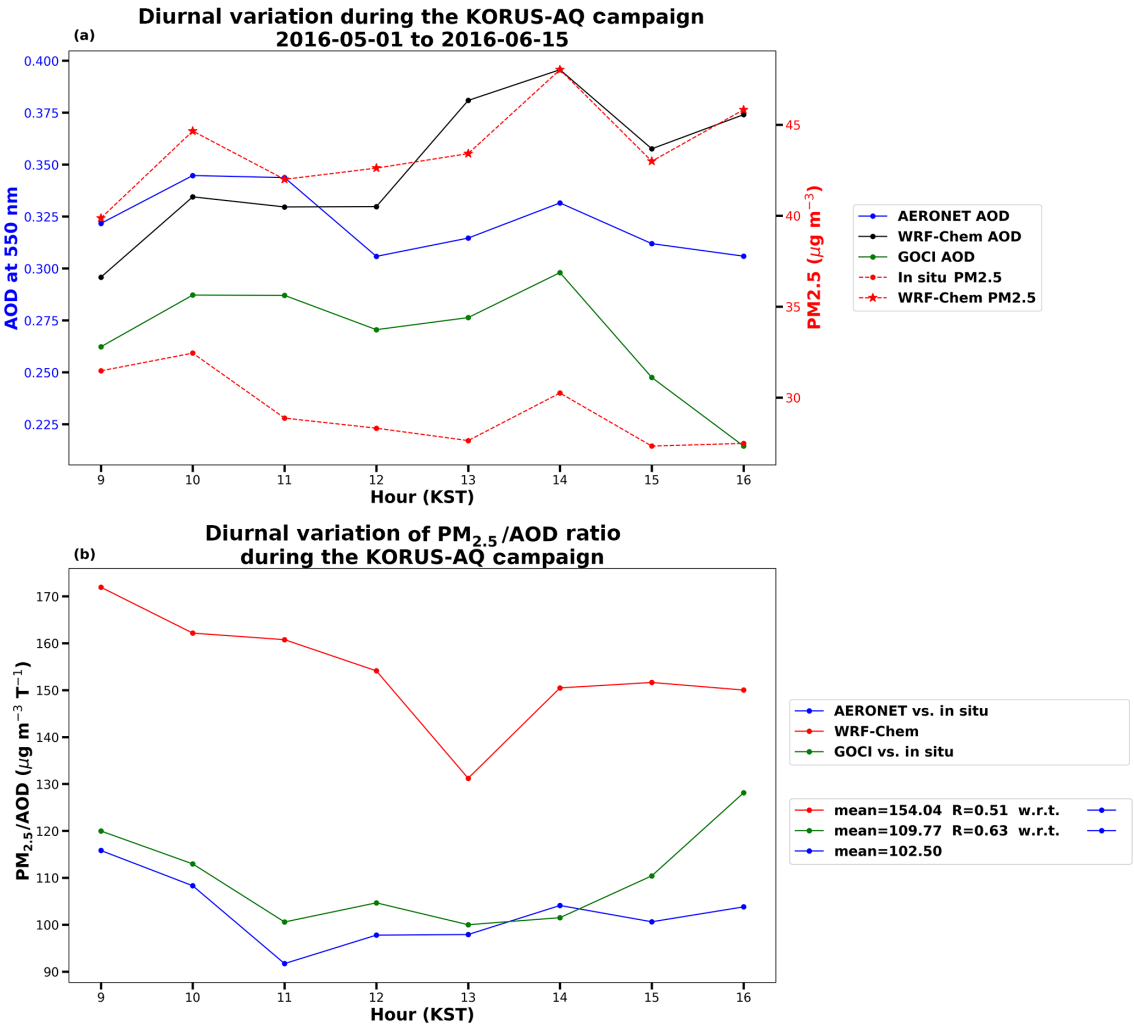

Figure 9. **(a)** The diurnal variations for AERONET, WRF-Chem, GOCI, and $PM_{2.5}$ for the sites in Table 2 using temporally and spatially matched data. **(b)** The diurnal variation of the WRF-Chem $PM_{2.5}$ / AOD ratio and observation-based counterparts (e.g., GOCI AOD / in situ $PM_{2.5}$ and AERONET AOD / in situ $PM_{2.5}$ ratio) for the average of the sites in Table 2 using temporally and spatially matched data. Also shown in the legend on the right-hand side of **(b)** are the mean value of these ratios and the correlation of GOCI / in situ and WRF-Chem hourly $PM_{2.5}$ / AOD ratios with respect to the that of AERONET / in situ, respectively.

AOD from geostationary satellites can be an integral part for deriving $PM_{2.5}$ values from AOD.

5 Summary and conclusions

By using all possible AERONET data in South Korea, the surface observation of $PM_{2.5}$, GOCI AOD, and WRF-Chem-simulated AOD during the KORUS-AQ field campaign in South Korea from April to June 2016, this study analyzed the diurnal variation of aerosol properties and surface $PM_{2.5}$ from surface observations and assessed their counterparts from models. In summary, the following conclusions were found.

Long-term AERONET data show that the climatological AOD diurnal variation is very similar amongst South Korean AERONET sites. Most see AOD maxima in the middle morning (10:00) and middle afternoon (14:00) and noontime AOD minima. Additionally, the coastal sites have lower average values near 0.3 at 550 nm while the inland sites have higher values near 0.4. The inland sites also experience the most AOD fluctuations during the day on the order of +20 % to −30 %. Analysis of the Ångström exponent shows a gradual increase throughout the day from 1.2 to 1.4.

Given there is a persistent diurnal variation of AOD and Ångström exponent in South Korea, we analyzed that, at a minimum, there should be more than 12 months of observation, and the coastal rural sites require observations twice as long (2 years) as that required for the inland urban sites, to characterize the climatology of diurnal variation of AOD at a statistically significant level. This suggests the distinct

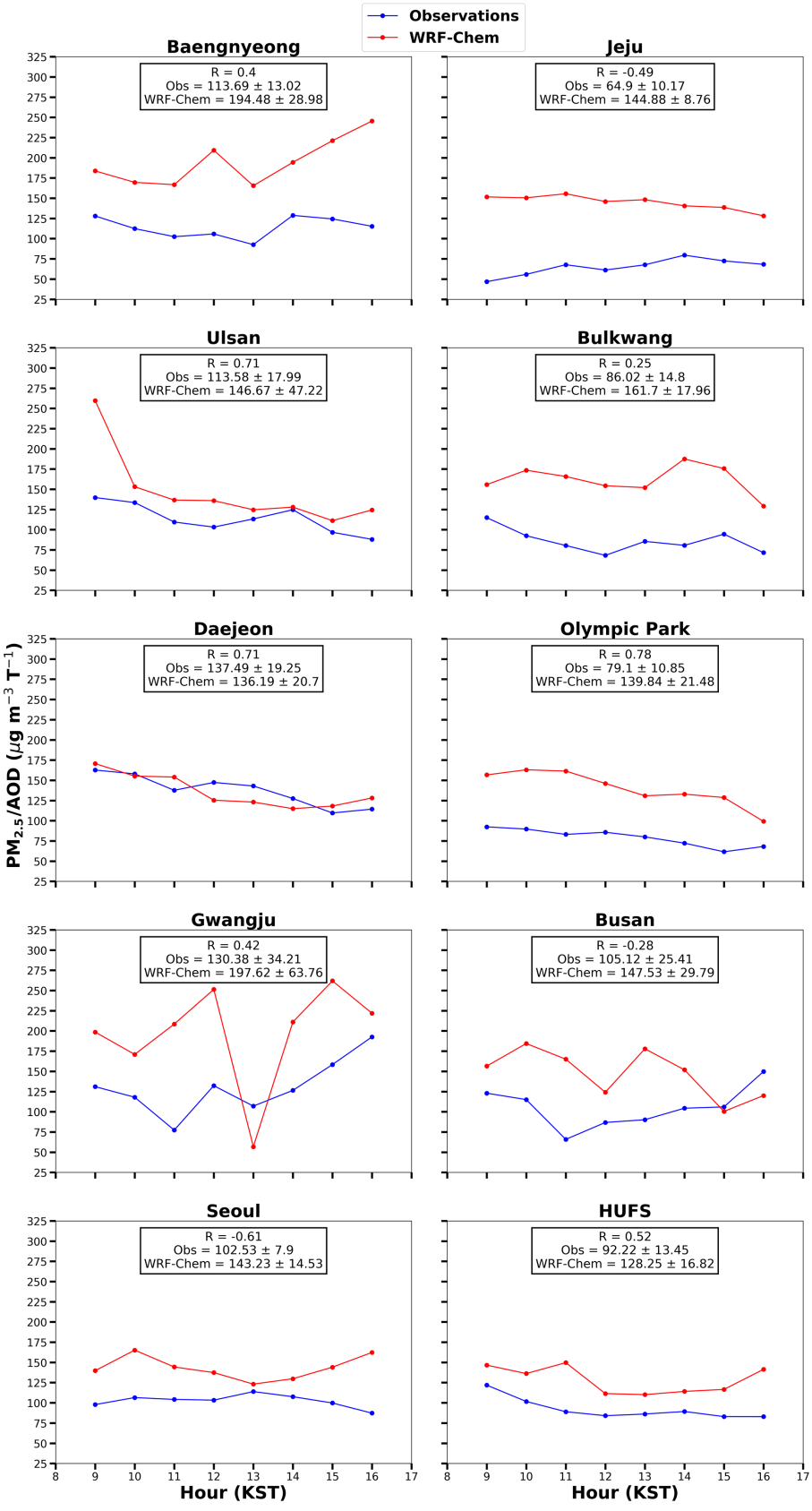

Figure 10. The diurnal variation of the observed (AERONET vs. in situ) and WRF-Chem $PM_{2.5}$ / AOD ratio for each site in Table 2 using temporally and spatially matched data. The ratio is in units of $\mu g\,m^{-3}\,t^{-1}$.

and persistent diurnal variation of aerosol properties in urban areas.

The AERONET and GOCI AOD had a linear correlation coefficient of (R) 0.8 and RMSE = 0.16 while the AERONET and WRF-Chem relationship had $R = 0.4$ and RMSE = 0.28, suggesting that AOD data retrieved from the GOCI satellite shows a closer agreement with AERONET AOD data than those from WRF-Chem model.

Analyses of 10 AERONET–surface-$PM_{2.5}$ paired sites show that the diurnal variation of $PM_{2.5}$ was $\sim 10\,\%$ throughout the day, with the exception of the Daejeon and HUFS sites having maxima at 08:00 KST (or peaks by 20 %) and values gradually decreasing and remaining steady for the remainder of the day after 12:00 KST. $PM_{2.5}$ daily-mean values were around $30\,\mu g\,m^{-3}$, which is still $20\,\mu g\,m^{-3}$ below the 24 h $PM_{2.5}$ air quality standard in South Korea but $5\,\mu g\,m^{-3}$ above the WHO recommendation. Overall, the day-to-day variation of mean $PM_{2.5}$ at all sites can be best described by the variation of hourly $PM_{2.5}$ data at noontime for each day and is least captured by the variation of $PM_{2.5}$ in the midnight hours.

AERONET, GOCI, WRF-Chem, and observed $PM_{2.5}$ data consistently show dual peaks for both AOD and $PM_{2.5}$, one at 10:00 KST and another at 14:00 KST. However, WRF-Chem shows the peak in afternoon is larger than the peak in the morning, which is the opposite of what GOCI and AERONET reveal. Consequently, WRF-Chem shows an increase in AOD and $PM_{2.5}$ from 09:00 to 16:00 KST, which contrasts with the deceasing counterparts in GOCI, AERONET, and observed $PM_{2.5}$. The analysis suggests that the diurnal profile of emissions in WRF-Chem may have a too-large skewness toward the afternoon.

The $PM_{2.5}$ / AOD ratio ranged from 60 to $120\,\mu g\,m^{-3}\tau^{-1}$ throughout the day, and no consistent pattern was seen at each of the 10 sites nor when further broken down into land classification. However, overall, the ratio in WRF-Chem is persistently larger than the observed counterparts by 30 %–50 %, and the observed ratio (from AERONET vs. in situ) shows lower values in late morning and afternoon. In contrast, the diurnal variation of the observed ratio is in better agreement with the ratio from GOCI vs. in situ, both showing the minimum at 11:00 KST and an increase toward the late afternoon. This highlights the need to use geostationary satellites to characterize AOD as a function of time as an integral part toward an improved estimate of surface $PM_{2.5}$.

By using rich datasets during KORUS-AQ, this study revealed there are persistent diurnal variations of AOD and surface $PM_{2.5}$ in South Korea. It is shown that the Korean GOCI satellite is able to consistently capture the diurnal variation of AOD, while WRF-Chem clearly has a deficiency in describing the relative change in the morning and afternoon. As a minimum of 1 year of observation is required to fully characterize the climatology of diurnal variation patterns of AOD, future field campaigns are recommended to have at least longer time periods of surface observations where AERONET and surface $PM_{2.5}$ networks can be collocated. Hence, future studies are needed to evaluate the statistical significance of our analysis of diurnal variation of $PM_{2.5}$ / AOD ratios with a longer record of observation data.

Data availability. AERONET data are downloaded from http://aeronet.gsfc.nasa.gov (NASA, 2018) and we thank all AERONET PIs in South Korea for collecting the data.

Author contributions. The paper is a result of the lead author's MS research work under the supervision of JW. JG, LCG, and CG helped in the data preparation and data analysis. MG, PS, and GC provided the WRF-Chem data. MC and JK provided the GOCI data. JW, JG, GC, and SJ designed the research. All authors participated in the process of writing the manuscript.

Competing interests. The authors declare that they have no conflict of interest.

Acknowledgements. This manuscript was part of author Lennartson's master's thesis and was in part supported by NASA's GEO-CAPE program and in part by the KORUS-AQ program (grant #: NNX16AT82G). GOCI aerosol product was supported by the development of the integrated data processing system for GOCI-II funded by the Ministry of Ocean and Fisheries, Korea. Elizabeth Lennartson and Jun Wang also thank Charles Stanier from the University of Iowa for his constructive comments.

Edited by: Leiming Zhang
Reviewed by: Chris Sioris and two anonymous referees

References

Aegerter, C., Wang, J., Ge, C., Irmak, S., Oglesby, R., Wardlow, B., Yang, H., You, J., and Shulski, M.: Mesoscale Modeling of the Meteorological Impacts of Irrigation during the 2012 Central Plains Drought, J. Appl. Meteorol. Climatol., 56, 1259—1283, 2017.

Ahmed, E., Kim, K. H., Shon, Z. H., and Song, S. K.: Long-term trend of airborne particulate matter in Seoul, Korea from 2004 to 2013, Atmos. Environ., 101, 125–133, 2015.

Barteneva, O. D., Dovgyallo, Y. N., and Polyakova, Y. A.: Investigations of the optical properties of the atmospheric surface layer, Proc. Main Geophys. Obs. (Trudy GGO), 36, 119–140, 1967 (in Russian).

Choi, J. K., Park, Y. J., Ahn, J. H., Lim, H. S., Eom, J., and Ryu, J. H.: GOCI, the world's first geostationary ocean color observation satellite, for the monitoring of temporal variability in coastal water turbidity, J. Geophys. Res.-Oceans, 117, C09004, https://doi.org/10.1029/2012JC008046, 2012.

Choi, M., Kim, J., Lee, J., Kim, M., Park, Y.-J., Jeong, U., Kim, W., Hong, H., Holben, B., Eck, T. F., Song, C. H., Lim, J.-H., and Song, C.-K.: GOCI Yonsei Aerosol Retrieval (YAER) algorithm

and validation during the DRAGON-NE Asia 2012 campaign, Atmos. Meas. Tech., 9, 1377–1398, https://doi.org/10.5194/amt-9-1377-2016, 2016.

Choi, M., Kim, J., Lee, J., Kim, M., Park, Y.-J., Holben, B., Eck, T. F., Li, Z., and Song, C. H.: GOCI Yonsei aerosol retrieval version 2 products: an improved algorithm and error analysis with uncertainty estimation from 5-year validation over East Asia, Atmos. Meas. Tech., 11, 385–408, https://doi.org/10.5194/amt-11-385-2018, 2018.

Christopher, S. A. and Gupta, P.: Satellite remote sensing of particulate matter air quality: the cloud-cover problem, J. Air Waste Manage. Assoc., 60, 596–602, 2010.

Edgerton, E. S., Hartsell, B. E., Saylor, R. D., Jansen, J. J., Hansen, D. A., and Hidy, G. M.: The southeastern aerosol research and characterization study, part 3: continuous measurements of fine particulate matter mass and composition, J. Air Waste Manage. Assoc., 56, 1325–1341, 2006.

EPA: Ambient Air Monitoring Strategy for State, Local, and Tribal Air Agencies AAMS for SLTs, 95 pp., 2008.

EPA: NAAQS table, available at: https://www.epa.gov/criteria-air-pollutants/naaqs-table (last access: 21 November 2017), 2016.

Fine, P. M., Chakrabarti, B., Krudysz, M., Schauer, J. J., and Sioutas, C.: Diurnal variations of individual organic compound constituents of ultrafine and accumulation mode particulate matter in the Los Angeles basin, Environ. Sci. Technol., 38, 1296–1304, 2004.

Gao, M., Carmichael, G. R., Wang, Y., Saide, P. E., Yu, M., Xin, J., Liu, Z., and Wang, Z.: Modeling study of the 2010 regional haze event in the North China Plain, Atmos. Chem. Phys., 16, 1673–1691, https://doi.org/10.5194/acp-16-1673-2016, 2016.

Ghim, Y. S., Chang, Y. S., and Jung, K.: Temporal and spatial variations in fine and coarse particles in Seoul, Korea, Aerosol Air Qual. Res., 15, 842–852, 2015.

Goldberg, D. L., Saide, P. E., Lamsal, L. N., de Foy, B., Lu, Z., Woo, J.-H., Kim, Y., Kim, J., Gao, M., Carmichael, G., and Streets, D. G.: A top-down assessment using OMI NO2 suggests an underestimate in the NOx emissions inventory in Seoul, South Korea during KORUS-AQ, Atmos. Chem. Phys. Discuss., https://doi.org/10.5194/acp-2018-678, in review, 2018.

Gong, S. L., Barrie, L. A., and Blanchet, J. P.: Modeling sea-salt aerosols in the atmosphere 1. model development, J. Geophys. Res.-Atmos., 102, 3805–3818, 1997.

Grell, G., Freitas, S. R., Stuefer, M., and Fast, J.: Inclusion of biomass burning in WRF-Chem: impact of wildfires on weather forecasts, Atmos. Chem. Phys., 11, 5289–5303, https://doi.org/10.5194/acp-11-5289-2011, 2011.

Grell, G. A., Peckham, S. E., Schmitz, R., McKeen, S. A., Frost, G., Skamarock, W. C., and Eder, B.: Fully coupled "online" chemistry within the WRF model, Atmos. Environ., 39, 6957–6975, 2005.

Guenther, A., Karl, T., Harley, P., Wiedinmyer, C., Palmer, P. I., and Geron, C.: Estimates of global terrestrial isoprene emissions using MEGAN (Model of Emissions of Gases and Aerosols from Nature), Atmos. Chem. Phys., 6, 3181–3210, https://doi.org/10.5194/acp-6-3181-2006, 2006.

Gupta, P., Christopher, S. A., Wang, J., Gehrig, R., Lee, Y., and Kumar, N.: Satellite remote sensing of particulate matter and air quality assessment over global cities, Atmos. Environ., 40, 5880–5892, 2006.

Han, Y. J., Kim, S. R., and Jung, J. H.: Long-term measurements of atmospheric $PM_{2.5}$ and its chemical composition in rural Korea, J. Atmos. Chem., 68, 281–298, 2011.

Hoff, R. M. and Christopher, S. A.: Remote sensing of particulate pollution from space: have we reached the promised land?, J. Air Waste Manage. Assoc., 59, 645–675, 2009.

Holben, B. N., Eck, T. F., Slutsker, I., Tanré, D., Buis, J. P., Setzer, A., Vermote, E., Reagan, J. A., Kaufman, Y. J., Nakajima, T, Lavenu, F., Jankowiak, I., and Smirnov, A.: AERONET – A federated instrument network and data archive for aerosol characterization, Remote Sens. Environ., 66, 1–16, 1998.

Kassianov, E., Barnard, J., Pekour, M., Berg, L. K., Michalsky, J., Lantz, K., and Hodges, G.: Do diurnal aerosol changes affect daily average radiative forcing?, Geophys. Res. Lett., 40, 3265–3269, 2013.

Kaufman, Y. J., Holben, B. N., Tanre, D., Slutsker, I., Smirnov, A., and Eck, T. F.: Will aerosol measurements from Terra and Aqua polar orbiting satellites represent the daily aerosol abundance and properties?, Geophys. Res. Lett., 27, 3861–3864, 2000.

Kaufman, Y. J., Tanre, D., and Boucher, O.: A satellite view of aerosols in the climate system, Nature, 419, 215–223, 2002.

Kuang, Y., Zhao, C. S., Tao, J. C., and Ma, N.: Diurnal variations of aerosol optical properties in the North China Plain and their influences on the estimates of direct aerosol radiative effect, Atmos. Chem. Phys., 15, 5761–5772, https://doi.org/10.5194/acp-15-5761-2015, 2015.

Lee, J., Kim, J., Song, C. H., Ryu, J. H., Ahn, Y. H., and Song, C. K.: Algorithm for retrieval of aerosol optical properties over the ocean from the Geostationary Ocean Color Imager, Remote Sens. Environ., 114, 1077–1088, 2010.

Lee, M.: An analysis on the concentration characteristics of $PM_{2.5}$ in Seoul, Korea from 2005 to 2012, Asia-Pac, J. Atmos. Sci., 50, 33–42, 2014.

Levin, Z., Joseph, J. H., and Mekler, Y.: Properties of sharav (khamsin) dust – comparision of optical and direct sampling data, J. Atmos. Sci., 37, 882–891, 1980.

Liu, Y., Park, R. J., Jacob, D. J., Li, Q. B., Kilaru, V., and Sarnat, J. A.: Mapping annual mean ground-level $PM_{2.5}$ concentrations using Multiangle Imaging Spectroradiometer aerosol optical thickness over the contiguous United States, J. Geophys. Res.-Atmos., 109, D22206, https://doi.org/10.1029/2004JD005025, 2004.

Liu, Y., Sarnat, J. A., Kilaru, A., Jacob, D. J., and Koutrakis, P.: Estimating ground-level $PM_{2.5}$ in the eastern united states using satellite remote sensing. Environ. Sci. Technol., 39, 3269–3278, 2005.

Ma, Z. W., Liu, Y., Zhao, Q. Y., Liu, M. M., Zhou, Y. C., and Bi, J.: Satellite-derived high resolution $PM_{2.5}$ concentrations in Yangtze River Delta Region of China using improved linear mixed effects model, Atmos. Environ., 133, 156–164, 2016.

Ministry of Environment: Air quality standards and air pollution level, available at: http://eng.me.go.kr/eng/web/index.do?menuId=252 (last access: 21 November 2017), 2016.

NASA: AERONET Aerosol Robotic Network, available at: https://aeronet.gsfc.nasa.gov/, last access: 25 September 2018.

Panchenko, M. V., Pkhalagov, Y. A., Rakhimov, R. F., Sakerin, S. M., and Belan, B. D.: Geophysical factors of the aerosol weather

formation in Western Siberia, Optica atmosphery i okeana, 12, 922–934, 1999 (in Russian).

Peterson, J. T., Flowers, E. C., Berri, G. J., Reynolds, C. L., and Rudisill, J. H.: Atmospheric turbidity over central North Carolina, J. Appl. Meteorol., 20, 229–241, 1981.

Pinker, R. T., Idemudia, G., and Aro, T. O.: Characteristic aerosol optical depths during the harmattan season on sub-sahara Africa, Geophys. Res. Lett., 21, 685–688, 1994.

Polivka, T., Hyer, E., Wang, J., and Peterson, D.: First global analysis of saturation artifacts in the VIIRS infrared channels and the effects of sample aggregation, IEEE Geosci. Remote Sens., 1262–1266, 2015.

Pope, C. A., Burnett, R. T., Thun, M. J., Calle, E. E., Krewski, D., Ito, K., and Thurston, G. D.: Lung cancer, cardiopulmonary mortality, and long-term exposure to fine particulate air pollution, JAMA-J. Am. Med. Assoc., 287, 1132–1141, 2002.

Qu, W., Wang, J., Zhang, X., Sheng, L., and Wang, W.: Opposite seasonality of the aerosol optical depth and the surface particulate matter concentration over the North China Plain, Atmos. Environ., 127, 90–99, 2016.

Querol, X., Alastuey, A., Rodriguez, S., Plana, F., Ruiz, C., Cots, N., Massague, G., and Puig, O.: PM 10 and $PM_{2.5}$ source apportionment in the Barcelona Metropolitan area, Catalonia, Spain, Atmos. Environ., 35, 6407–6419, 2001.

Schuster, G. L., Dubovik, O., and Holben, B. N.: Angstrom exponent and bimodal aerosol size distributions, J. Geophys. Res.-Atmos., 111, D07207, https://doi.org/10.1029/2005JD006328, 2006.

Smirnov, A., Holben, B. N., Eck, T. F., Dubovik, O., and Slutsker, I.: Cloud-screening and quality control algorithms for the AERONET database, Remote Sens. Environ., 73, 337–349, 2000.

Smirnov, A., Holben, B. N., Eck, T. F., Slutsker, I., Chatenet, B., and Pinker, R. T.: Diurnal variability of aerosol optical depth observed at AERONET (Aerosol Robotic Network) sites, Geophys. Res. Lett., 29, 2115, https://doi.org/10.1029/2002GL016305, 2002.

Song, J., Xia, X., Che, H., Wang, J., Zhang, X., and Li, X.: Daytime variation of aerosol optical depth in North China and its impact on aerosol direct radiative effects, Atmos. Environ., 182, 31–40, 2018.

Sun, Y. L., Wang, Z. F., Fu, P. Q., Yang, T., Jiang, Q., Dong, H. B., Li, J., and Jia, J. J.: Aerosol composition, sources and processes during wintertime in Beijing, China, Atmos. Chem. Phys., 13, 4577–4592, https://doi.org/10.5194/acp-13-4577-2013, 2013.

van Donkelaar, A., Martin, R. V., Brauer, M., Kahn, R., Levy, R., Verduzco, C., and Villeneuve, P. J.: Global estimates of ambient fine particulate matter concentrations from satellite-based aerosol optical depth: development and application, Environ. Health Persp., 118, 847–855, 2010.

Wang, J.: Clint Aegerter, Xiaoguang Xu, and J. J. Szykman, Potential application of VIIRS Day/Night Band for monitoring nighttime surface $PM_{2.5}$ air quality from space, Atmos. Environ., 124, 55–63, 2016.

Wang, J. and Christopher, S. A.: Intercomparison between satellite-derived aerosol optical thickness and $PM_{2.5}$ mass: implications for air quality studies, Geophys. Res. Lett., 30, 2095, https://doi.org/10.1029/2003GL018174, 2003.

Wang, J. and Christopher, S. A.: Mesoscale modeling of central American smoke transport to the United States, 2: Smoke regional radiative impacts on surface energy budget and boundary layer evolution, J. Geophys. Res., 111, D14S92, https://doi.org/10.1029/2005JD006720, 2006.

Wang, J., Christopher, S. A., Brechtel, F., Kim, J., Schmid, B., Redemann, J., Russell, P. B., Quinn, P., and Holben, B. N.: Geostationary satellite retrievals of aerosol optical thickness during ACE-Asia, J. Geophys. Res.-Atmos., 108, 8657, https://doi.org/10.1029/2003JD003580, 2003a.

Wang, J., Christopher, S. A., Reid, J. S., Maring, H., Savoie, D., Holben, B. N., Livingston, J. M., Russell, P. B., and Yang, S. K.: GOES 8 retrieval of dust aerosol optical thickness over the Atlantic Ocean during PRIDE. J. Geophys. Res.-Atmos., 108, 8595, https://doi.org/10.1029/2002JD002494, 2003b.

Wang, J., Xia, X. G., Wang, P. C., and Christopher, S. A.: Diurnal variability of dust aerosol optical thickness and Angstrom exponent over dust source regions in China, Geophys. Res. Lett., 31, L08107, https://doi.org/10.1029/2003GL019580, 2004.

Wang, J., Christopher, S. A., Nair, U. S., Reid, J. S., Prins, E. M., Szykman, J., and Hand, J. L.: Mesoscale modeling of Central American smoke transport to the United States, 1: "top-down" assessment of emission strength and diurnal variation impacts, J. Geophys. Res., 11, D05S17, https://doi.org/10.1029/2005JD006416, 2006.

WHO: Air quality guidelines global update 2005: particulate matter, ozone, nitrogen dioxide and sulfur dioxide, WHO Report WHO/SDE/PHE/OEH/06.02, 20 pp., 2006.

Wittig, A. E., Anderson, N., Khlystov, A. Y., Pandis, S. N., Davidson, C., and Robinson, A. L.: Pittsburgh air quality study overview, Atmos. Environ., 38, 3107–3125, 2004.

Xu, J.-W., Martin, R. V., van Donkelaar, A., Kim, J., Choi, M., Zhang, Q., Geng, G., Liu, Y., Ma, Z., Huang, L., Wang, Y., Chen, H., Che, H., Lin, P., and Lin, N.: Estimating ground-level $PM_{2.5}$ in eastern China using aerosol optical depth determined from the GOCI satellite instrument, Atmos. Chem. Phys., 15, 13133–13144, https://doi.org/10.5194/acp-15-13133-2015, 2015.

Yoo, J.-M., Jeong, M.-J., Kim, D., Stockwell, W. R., Yang, J.-H., Shin, H.-W., Lee, M.-I., Song, C.-K., and Lee, S.-D.: Spatiotemporal variations of air pollutants (O_3, NO_2, SO_2, CO, PM_{10}, and VOCs) with land-use types, Atmos. Chem. Phys., 15, 10857–10885, https://doi.org/10.5194/acp-15-10857-2015, 2015.

Zang, Z. L., Wang, W. Q., You, W., Li, Y., Ye, F., and Wang, C. M.: Estimating ground-level $PM_{2.5}$ concentrations in Beijing, China using aerosol optical depth and parameters of the temperature inversion layer, Sci. Total Environ., 575, 1219–1227, 2017.

Zhao, C., Liu, X., Leung, L. R., Johnson, B., McFarlane, S. A., Gustafson Jr., W. I., Fast, J. D., and Easter, R.: The spatial distribution of mineral dust and its shortwave radiative forcing over North Africa: modeling sensitivities to dust emissions and aerosol size treatments, Atmos. Chem. Phys., 10, 8821–8838, https://doi.org/10.5194/acp-10-8821-2010, 2010.

Zheng, Y. X., Zhang, Q., Liu, Y., Geng, G. N., and He, K. B.: Estimating ground-level $PM_{2.5}$ concentrations over three megalopolises in China using satellite-derived aerosol optical depth measurements, Atmos. Environ., 124, 232–242, 2016.